View metadata, citation and similar papers at core.ac.uk

brought to you by CORE

provided by The University of North Carolina at Greensboro

HUMAN IMPACT ON THE SILICA CYCLE: REDUCTION OF DISSOLVED SILICA INPUTS INTO THE OCEAN AS A RESULT OF THE INCREASING IMPERVIOUS COVER.

Socratis Loucaides

A Thesis Submitted to the
University of North Carolina at Wilmington in Partial Fulfillment
Of the Requirements for the Degree of
Master of Science In Marine Science

University of North Carolina at Wilmington

2003

Approved by

Advisory Committee

_____ _____

_____ _____

Chair

Accepted by

_____

Dean, Graduate School

TABLE OF CONTENTS

ABSTRACT iii

ACKNOWLEDGMENTS v

DEDICATION vi

LIST OF TABLES vii

LIST OF FIGURES viii

INTRODUCTION 1

Background 1

Dissolved silica cycle 3

Hydrology 7

Impervious cover 8

HYPOTHESIS/GOALS 12

METHODOLOGY 13

Site description and GIS analysis 13

Sample collection and analysis 19

RESULTS 31

Baseflow 31

Rain events 34

DISCUSSION 45

Baseflow 45

Rain events 47

REFERENCES 55

ABSTRACT

Frequent harmful algal blooms in coastal waters have been linked to increasing nitrogen (N) and phosphorous (P) loadings. Recent studies, however, have shown that dissolved silica (DSi) depletion in natural waters can be an important if not the most important factor that triggers these events. Long term hydrologic and water quality data give signs of significant human impact on the silicon cycle. More specifically, by altering the hydrology of the land, humans may have reduced the amount of DSi that reaches the oceans through freshwater streams. This study examined the hypothesis that a watershed with more impervious cover discharges less DSi per unit watershed than a more undisturbed watershed.

DSi discharge data were collected from 2 different freshwater streams with watersheds of different % impervious cover during 5 non-rain and 4 rain events. The stream with higher impervious cover discharged higher DSi per unit watershed during non-rain events. During intense rain events the more impervious watershed rapidly released stormwater as low-DSi runoff while the less impervious watershed released less runoff and more DSi per unit watershed. During low intensity rain events the less impervious watershed released no runoff while DSi discharge increased. The more impervious watershed released runoff even during the lightest event. Using the CN method developed by the Soil Conservation Service, it was found that a more impervious watershed not only produced more runoff than a less impervious watershed, but it also produced runoff more often. Higher volume of runoff can cause short term DSi dilution during rain events as well as long-term reduction of DSi inputs to coastal

waters. According to the CN method a long-term reduction of DSi loads is taking place in response to increasing impervious cover.

Since diatom primary production is possibly the most important link of the marine food chain, and since diatom growth is DSi limited, reduction of the coastal oceans' silica budget may have negative impacts on all levels of the food chain.

ACKNOWLEDGMENTS

Special thanks to my advisor and graduate committee chair Dr. Lawrence Cahoon for his guidance and support throughout the project, and graduate committee members, Dr. Joan Willey, Dr. Eric Henry, and Dr. Lynn Leonard for their time and expertise.

Most of all I thank my family for supporting and encouraging every step of my academic career abroad; thanks for letting me be away for so long; and friends for their constant support and encouragement.

DEDICATION

This thesis is dedicated to my parents, without whom any degree would not have been possible. Thanks for helping me accomplish my dreams.

LIST OF TABLES

Table Page

1. Characteristics of each watershed estimated from GIS data 17

2. Soil types present in each watershed and their characteristics (USDA, 1986) ... 18

3. Means and ANOVA results for the various parameters calculated from non-rain event data 32

4. Total water and DSi discharge over each rain event with per unit watershed calculations incorporated 39

5. Stormwater discharge data for the two streams with baseflow discharge subtracted 44

6. Total loads discharged by each watershed during a 2-year period (2001-2002) estimated using the CN method 46

LIST OF FIGURES

Figure Page

1. The sub-watersheds studied are part of the Bradley Creek watershed located on the coast of New Hanover County, NC 14

2. Map of the study area showing the two watersheds and two streams studied including the location of the groundwater well used for groundwater sampling. Shaded area represents the impervious cover 15

3. Map showing the sampling and dye injection sites close to the convergence point of the two streams between stations 1 and 2 20

4. Streamflow hydrograph separated into the three sections..... 27

5. CN curves for each watershed calculated using 2001-2002 daily rainfall data. CN curves represent the relationship between rainfall and runoff production on a watershed 30

6. DSi concentrations of the two streams and groundwater wells during non-rain events. (Stream A: mean=72.4μM, std dev=4.38, n=120. Stream B: mean=67.6μM, std dev=2.07, n=55. Shallow well: mean=66.3μM, std dev=4.80, n=6. Deep well: mean=136.7μM, std dev=30.9, n=6)..... 35

7. DSi concentration response to streamflow increase during a rain event (July 23-24, 2003) in the two streams (Rain=2.34cm). a.) Stream A b.) Stream B36

8. DSi concentration response to streamflow increase during a rain event (June 4-5, 2003) in the two streams (Rain=0.35cm). a.) Stream A b.) Stream B..... 37

9. DSi discharge for each stream during two different rain events. a.) April 23-24, 2003 (Rain=2.34cm). b.) June 4-5, 2003 (Rain=0.35) 38

10 a.) Relationship between total DSi discharged by each km^3 of watershed and total precipitation for each rain event. b.) Relationship between total water discharged and total precipitation for each rain event..... 41

11. a.) Relationship between total DSi discharged by each km^2 of watershed and total precipitation for each rain event. b.) Relationship between total water discharged and total precipitation for each rain event..... 42

12. a.) Relationship between total DSi discharged and total precipitation for each rain event. b.) Relation between total water discharged and total precipitation for each rain event 43

13. Rainfall frequency distribution chart for 2001-2002 rain events 52

INTRODUCTION

Background

Increases in frequency and intensity of harmful algal blooms have been observed worldwide during the last few decades (Smayda, 1990; Anderson, 1997). Relatively new phenomena to the northeastern United States, including paralytic shellfish poisoning caused by toxic dinoflagellates of the genus *Alexandrium*, are now recurrent and widespread (Anderson, 1997). Altered environmental parameters (i.e. nutrient cycles, climate changes, etc) may have created, in many cases, conditions that can specifically promote blooms of noxious algal species (Bricelj and Lonsdale, 1997). Toxic algal outbreaks, including the well known noxious dinoflagellate *Pfiesteria piscicida,* are commonly associated with high nitrogen and phosphorus inputs that follow intense rainfall events (Burkholder and Glasgow, 1997). Even though a cause and effect relationship may seem to exist between N/P inputs and harmful algal bloom occurrences, the actual cause of these events may be a different one. High nutrient inputs may not always lead to these types of events.

Harmful algal blooms are primarily flagellate events (Sournia, 1995). Diatom blooms, in contrast, are usually very beneficial and valuable to the ecosystem because they enrich the base of the food web. Diatoms are abundant planktonic and benthic photoautotrophs (Officer and Ryther, 1980; Sundbäck and Jonsson, 1988; Nilsson et al., 1991) that unlike most other algal species need dissolved silica (DSi) to synthesize their solid silica frustules (Busby and Lewin, 1967; Davis, 1976). In terms of contributions to global primary productivity, diatoms are among the most important aquatic photosynthesizers, dominating the phytoplankton of cold, nutrient-rich waters,

such as upwelling areas of the oceans, shallow coastal waters and newly circulated lakes (Graham and Wilcox, 2000).

In areas of stratification, phytoplankton assemblages show a regular successional pattern from diatom- to dinoflagellate-dominated (Garrison, 1979; Schrader 1981). This shift from diatom to dinoflagellate plankton species can be explained by the silica depletion hypothesis advanced in the 1970s (Schelske and Stoermer, 1971, 1972). According to this hypothesis, increased loads of nitrogen and phosphorous increase primary production as well as DSi utilization by diatoms. The increased utilization of DSi can then cause DSi depletion to the surface layers leading to DSi-limited diatom growth (Schelske, 1999). Brzezinski (1985) determined that marine diatoms average a nitrogen to silicon molar ratio (N:Si) of approximately 1. In addition, studies have shown that unlike the diatoms' ability to store nitrogen, accumulation of DSi immediately prior to cell division is necessary, leaving diatoms more susceptible to DSi than N limitation (Busby and Lewin, 1967, Davis 1976, Doering et al., 1989). Since size-based diatom growth rates exceed dinoflagellate rates by ~3-fold (Banse, 1982; Smayda, 1997), during high nutrient inputs diatoms will outcompete dinoflagellate blooms as long as DSi does not become limited. Havskum et al. (2003) demonstrated that in mesocosms enriched with N, P, glucose as well as DSi, bacterial and flagellate growth was inhibited because mineral nutrients were channeled into fast growing diatoms. Declining Si:N and Si:P ratios have been observed in many locations including the North Sea (Paerl, 1997), and the Mississippi plume (Rabalais et al., 1996). These ratios may reflect decreasing availabilities of DSi relative to N and P as well as increases in N and P loadings. Where as some workers suggest that the reduction of

these ratios is a result of increasing N and P inputs, other evidence suggests that a long-term reduction of bioavailable silica inputs into coastal waters is also taking place (Rabalais et al., 1996; Treguer et al., 1995). The total annual riverine load of DSi into the Gulf of Riga was estimated by Laznik et al. (1999) to be 65,000 tons, about half as much as it was estimated by Auninsh (1968) about 29 years earlier and about 7,500 tons less than was estimated by Laznik et al. (1988) twelve years earlier. Rabalais et al. (1996) also observed long-term changes in nutrient proportions in the surface waters of the northern Gulf of Mexico adjacent to the Mississippi River delta. It appeared that P and N deficiency have decreased over time while Si deficiency has increased. A shift in phytoplankton species composition was also observed. Data suggested that a shift in dominant diatom composition, toward more lightly silicified species, occurred between 1955 and 1973. On the Louisiana shelf, noxious non-diatom species are now present but were either absent before or have over the years increased in relative abundance (Rabalais et al., 1996).

Dissolved Silica cycle

Most of the dissolved silica available in coastal waters is carried from uplands by freshwater after being released mostly by chemical weathering of rocks and soils. Very little is derived from the weathering of seashore sands (Iler, 1979). Chemical weathering in nature occurs when water and other natural solvents react with rock material releasing elements available for uptake by the biota. The process consists of a series of chemical reactions with rates strongly influenced by the local climate. Warmer and wetter climates significantly enhance the weathering process (Peltier, 1950). The

dominant form of chemical weathering is driven by the formation of carbonic acid in the soil solution:

$$H_2O + CO_2 \Leftrightarrow H_2CO_3 \Leftrightarrow H^+ + HCO_3^-$$

The partial pressure of CO_2 in the soil depends on the amount of decomposing organic mater in the soil and the amount of CO_2 released by plant roots. Organic acids released by plant roots, bacteria or fungi are also known to enhance weathering rates (Garrels and MacKenzie, 1971).

Silicate minerals are divided into two classes, the ferromagnesian series and the felsic series, based on the presence of Mg or Al in the crystal structure, respectively. The rates of chemical weathering of primary silicate minerals tend to follow a reverse sequence of their formation during the original cooling and crystallization of rock. Minerals that condensed first (i.e. olivine) are the most susceptible to weathering reactions. These minerals are formed through rapid and early crystallization at high temperatures and contain few bonds that link the units of their crystalline structure. Primary minerals of this sort are those in which various cationic elements or trace metals are substituted in the silicate crystal structure (i.e. $FeMgSiO_4$). In comparison, quartz is a very simple silicate mineral consisting only of silicon and oxygen atoms. Because of its crystalline properties, quartz is very resistant to weathering.

During the process of weathering of silicate minerals, primary minerals are transformed to secondary minerals by the removal of DSi and other ions. In the case of albite ($NaAlSi_3O_8$), carbonic acid attacks the mineral removing the sodium cation and soluble silica:

$$2NaAlSi_3O_8 + 2H_2CO_3 + 9H_2O \rightarrow 2Na^+ + 2HCO_3^- + 4H_4SiO_4 + Al_2Si_2O_5(OH)_4$$

primary mineral — Albite; secondary mineral — Kaolinite

The secondary mineral obtained, Kaolinite, can undergo further weathering releasing more silicic acid into the water medium (Schlesinger, 1991):

$$Al_2Si_2O_5(OH)_4 + 5H_2O \rightarrow 2H_4SiO_4 + Al_2O_3 \cdot 3H_2O$$

kaolinite — silicic acid

Rainwater that infiltrates through the ground becomes the weathering agent as well as the medium in which silicic acid travels through the ground to eventually feed streams and rivers. The dissolution of amorphous silica in fresh water varies depending on the nature of the silicate mineral. Different solubility values experimentally obtained by several workers have led to confusion in the scientific community. As Iler (1979) explained, however, the solubility of a particular sample of silicate mineral depends on the average grain size of the sample, on the traces of impurities inside the mineral or adsorbed on its surface during dissolution, as well as on the state of the mineral's internal hydration. Even though a single figure for the solubility of amorphous silica does not exist, experimental solubility values for freshwater vary between 1600 to 2000 μM (Iler, 1979). Over 2000 μM, polymerization of silicic acid may take place forming polysilicic acids that are mostly unavailable to diatoms. Levels exceeding 2000 μM, however, are rarely found in natural waters. The process of silica dissolution is a very slow process, so only water that spends considerable amounts of time percolating through the soil can be enriched with silicic acid. Dissolved silica concentrations in river waters vary over the length of the channel. Runoff water associated with rain events can

cause dilution of the silica solution in stream waters where as groundwater inputs, usually rich in DSi, tend to enhance DSi concentrations. Runoff is usually poor in DSi since it is mostly rainwater, known to contain no significant amounts (<1 μM) of DSi (Cahoon et al., 2003).

Increased uptake of DSi by the biota, including diatoms and numerous aquatic plants, has been a popular explanation for the observed decrease of riverine dissolved silica discharge to coastal waters (Rabalais et al., 1996, Krauskoph, 1956; Kennedy, 1971). Drever and Zobrist (1992), however, contend that uptake by biota does not significantly affect DSi concentrations in streams and rivers. Uptake by biota can be significant only in areas with low flow rates (lentic environments) where diatoms and aquatic plants can sufficiently reproduce. In estuaries, for example, biological uptake can be highly significant with removals ranging from 4% in tropical rivers up to 50% in temperate rivers (Drever and Zobrist, 1992).

Most of the dissolved silica lost as biogenic matter eventually redissolves with only 3% average preservation ratio (burial/gross production). Since this ratio is relatively small, the reduction observed by many in silicic acid inputs into the ocean may also be a result of anthropogenic perturbations of the riverine source (Treguer, 1995). The construction of reservoirs in rivers in conjunction with increasing N and P inputs can significantly decrease DSi transports. Storage lakes, especially those with high nutrient inputs, can become major sinks of dissolved silica (Wahdy, 1982).

Even though the focus of the scientific community concerned with the issue of DSi limitation has been towards biological uptake, in this study the focus is oriented

towards an earlier step of the silica cycle: the interaction of the hydrological cycle with silica flux into surface waters.

Hydrology

Groundwater movement is usually very slow. During a natural water cycle, water spends most of its time in the soil. Although it spends a few days in the atmosphere and a few days or weeks in surface water bodies, it may spend weeks and months moving through the soil. This slow movement through the soil allows the water to recharge with DSi as the slow weathering reactions take place (Manning, 1997). The movement of water into and through the soil depends on the physical and hydraulic properties of the soil. Physical properties include soil bulk density, organic matter content, clay type and particle size where hydraulic properties include water content, water retention characteristics, hydraulic conductivity and hysteresis. These properties can be estimated for each particular type of soil using soil infiltration parameter charts (Rawis and Brakensiek, 1983) or they can also be determined experimentally. As soil becomes saturated with water its capacity to absorb more water steadily declines, producing more storm runoff.

Impervious Cover

Storm runoff results from short duration, high intensity rainfall or long duration, low intensity rainfall. In urbanized paved areas however, any amount of rainfall can create surface runoff. The potential of an area to produce storm runoff as well as the fraction of rainfall that will become runoff depend on the runoff coefficient determined by

the soil properties mentioned earlier as well as the topography of the area. In urbanized areas, on the other hand, the major factor that determines the magnitude of the runoff coefficient is the percent impervious cover. The US Nationwide Urban Runoff Program (NURP) reported in 1983 after a 2-year data collection effort that the observed runoff coefficient increases as the percent impervious surface increases in a watershed (USEPA, 1983). Impervious cover has also been recognized as a major factor affecting stream hydrology and water quality. The Center for Watershed Protection developed a model based on more than forty scientific studies that relates the percent impervious cover of a watershed to the degree of stream degradation (CWP, 1998). According to this model, watersheds with impervious cover as low as 10% may have negative impacts on the stream's quality. Impervious cover and urban land use alterations, including soil compaction and storm drain construction, alter infiltration rates and increase runoff velocities and the efficiency with which water is delivered to streams resulting in an increase of runoff volumes. Schueler (1987) demonstrated that runoff coefficients were found to be strongly correlated with impervious cover at 44 sites nationwide. In Australia, Neller (1988) also observed that an urban watershed produced more than seven times as much runoff as a similar rural watershed. Increased peak discharge rate is another sign of a stream impacted by impervious cover. Doll et al. (2000) compared 18 urban streams with 11 rural streams in the North Carolina Piedmont and found that unit area peak discharge was always greater in urban streams. Twenty percent impervious cover can cause, according to seven nationwide studies, the mean annual flood to double (Leopold 1968). Bankfull flow frequency also seems to increase with increasing impervious cover. Leopold (1968), using hydrologic data from a

nine-year period, estimated that a 50% imperviously covered watershed could create bankfull flows 4 times more often than normal. Not only frequency, but also duration of bankfull flow was observed to increase in response to urbanization. MacRae (1996) observed that the exceedence of bankfull flows increased by a factor of 4.2 once watershed impervious cover exceeded 30%.

When porous land is converted to impervious cover, a greater fraction of annual rainfall is converted to surface runoff, and a smaller volume recharges the groundwater. The increase of surface runoff leads to higher and longer peak flows and lower base flows during dry conditions (Cappiella et al., 2001). Klein (1979) reported an inverse relationship between impervious cover and baseflow. Spinello and Simmons (1992) demonstrated that baseflow in two urban Long Island streams declined seasonally as a response to increasing impervious cover.

Urbanization can alter the hydrologic regime of a watershed in other ways as well. Simmons and Reynolds (1982) discovered that even though impervious cover can significantly reduce the percent base flow of a stream, a much greater reduction of the base flow fraction can be caused by the way wastewater of an area is managed. This was observed after examining a 20-year long hydrograph data set taken from several streams in Long Island. Their study showed that the base flow fraction of total streamflow of streams fed by urbanized “sewered” watersheds declined from 87% in 1948 to 13% in 1969. In comparison the base flow fraction for two streams fed by an urbanized watershed without a central sewer system installed declined from 88% in 1948 to 81% in 1969 (Simmons and Reynolds, 1982). Sewer systems collect water withdrawn from residential or community wells and release it directly into rivers or

oceans. Areas with septic tanks installed do not experience the same base flow reductions since the water withdrawn from the groundwater aquifer is returned to the same area. Less reduction of base flow may also occur in areas where although central sewer system is used the water supply is not local groundwater but surface water from a different area or in rare cases desalinated seawater.

Impervious cover is also known to have physical impacts on the stream's morphology. Morse (2001) showed that increasing impervious cover could increase erosion rates in stream channels. Whereas in rural streams channel erosion accounts for only 5 to 20% of the annual sediment yield (Collins et al., 1997 and Walling and Woodward, 1995), 60 to 75% of the sediment yield of urban watersheds is derived from channel erosion (Trimble, 1997 and Dartingunave et al., 1997). According to a recent report by the Center of Watershed Protection [CWP] (2003), impervious cover is also known to cause channel incision, stream embeddedness, loss of large woody debris, changes in pool/riffle structure, loss of riparian cover, reduced channel sinuosity, as well as warming of streamwater temperatures (CWP, 2003).

Because low order streams are the first aquatic systems to receive stormwater runoff, their water quality is often compromised by the numerous pollutants impervious surfaces collect. Stormwater pollutants often include sediments, trace metals, hydrocarbons, organic carbon, pesticides, bacteria and pathogens, and nutrients (CWP, 2003). Even though nitrogen and phosphorous are essential nutrients for aquatic systems, in excess concentrations they can exert a negative impact on receiving waters. Research suggests that lawns are the major source of N and P in urban streams. Lawn runoff concentrations can be as much as four times greater than other

urban sources. While the nutrient concentrations of impervious cover runoff is lower than lawns' the volume of runoff is significantly higher bringing impervious cover up as the second most important source after lawns (Bannerman et al., 1993; Steuer et al., 1997 and Waschbusch et al., 2000).

Otto et al. (2002) presented the argument that the increasing percent of impervious cover and urban sprawl may be responsible for depleting water supplies and water shortages suffered in the past few decades. Based on a model using USGS data and other published information Otto et al. (2002) estimated how much groundwater recharge may be lost due to impervious cover runoff in the top 20 sprawling metropolitan areas. In Atlanta, GA, for example, they estimated that between 56.9 and 132.8 billion gallons of groundwater infiltration may have been lost in 1997 compared to 15 years earlier (Otto et al., 2002).

Groundwater that feeds streams during base flow conditions accounts for about 30-40% of the total water discharged by streams in the United States (Manning, 1997). This fraction of total water discharge is responsible for most of the dissolved silica that enriches the coastal waters; thus by increasing the percent impervious cover the amount of dissolved silica that flows to the ocean every year may be proportionally reduced.

HYPOTHESIS/GOALS

The effects of percent impervious cover on stream hydrology are well documented. Because the DSi cycle depends directly on hydrology, an indirect effect on stream DSi discharge was therefore expected. Since the cumulative base flow, as a

fraction of total streamflow, decreases as impervious cover increases on a watershed, this study hypothesized that the net DSi discharge per unit watershed volume of a stream also proportionally declines with increasing impervious cover. Furthermore, a watershed with higher percent impervious cover was expected, according to this hypothesis, to contribute less DSi per unit watershed volume or area than a watershed with less impervious cover.

In order to test this hypothesis this study examined weather the DSi released by a unit of watershed into a stream over a period of time was a function of the fraction of its area that was imperviously covered. A watershed with less impervious cover was expected to release more DSi per unit volume than a watershed with a higher percent of impervious cover during rain or non-rain events.

METHODOLOGY

Site description and GIS analysis

Two watersheds with different percent of impervious cover were chosen for this study. Both are sub-watersheds of the Bradley Creek watershed, one of the most heavily impacted watersheds in New Hanover County. The Bradley Creek watershed (Figure 1) occupies an area of 24.48 km^2. By 2000, 77.8% of its total area was developed and occupied by 13,657 residents (Mallin et al., 2003). The two sub-watersheds chosen for this study discharge into two streams that converge to form the upper branch of Bradley Creek, which discharges into the Atlantic Intracoastal Waterway. The larger of the two watersheds, watershed A (wA) has an area of 1.87 km^2 in which 49.2% is covered by impervious surfaces including houses, roads and strip mall parking lots in the area (Figure 2).

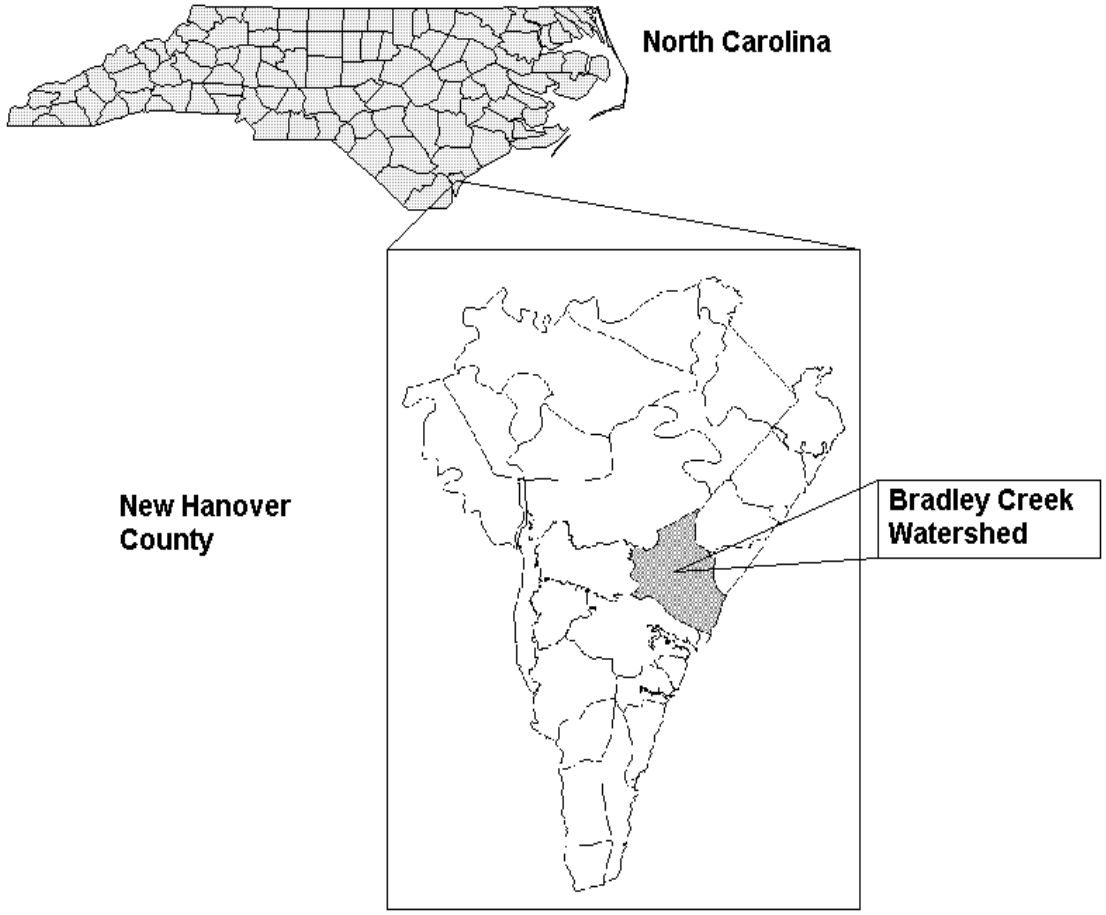

Figure 1. The sub-watersheds studied are part of the Bradley Creek watershed located on the coast of New Hanover County, NC.

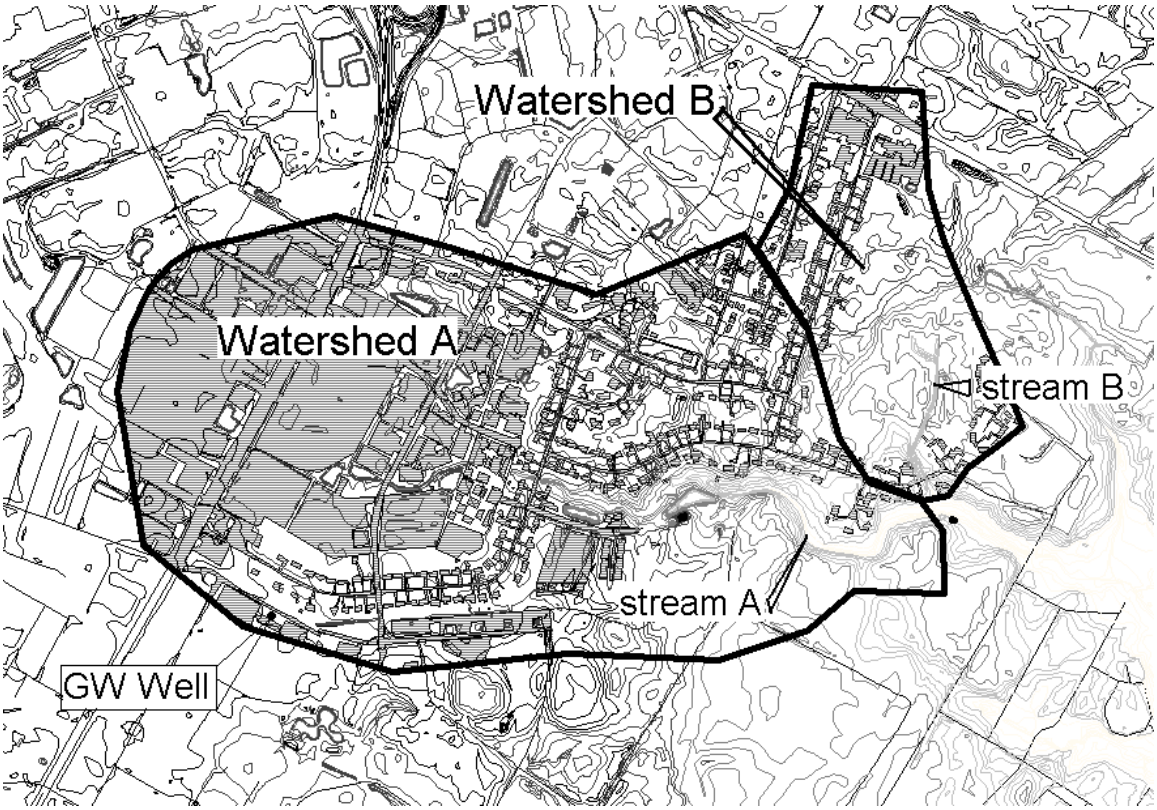

Figure 2. Map of the study area showing the two watersheds and two streams studied including the location of the groundwater well used for groundwater sampling. Shaded area represents impervious cover.

Watershed B (wB) has an area 4.5 times smaller than wA (0.41 km^2) and only 17.1% of its area is imperviously covered by mostly single-family homes and roads. The rest of wB is occupied by a golf course and other relatively pervious surfaces. All houses in either watershed are on public water supply and central sewer system. Attributes for the two watersheds are summarized in Table 1. In this study a watershed is defined as the segment of land responsible for the water supply of a stream. Since the watersheds for each stream have not been previously defined, GIS topographic datasets were used to define the corresponding watershed for each stream with the help of ArcView® GIS 3.2 software. Digital aerial photographs taken in 2002 were used, along with USGS elevation data, to define the boundary of each watershed. The volume of each aquifer that may supply each stream with groundwater was also calculated using GIS elevation data. Aquifer volume in this case was defined as the volume of land within each watershed boundary and above the elevation of each sampling site. GIS data were provided by the New Hanover County's Planning Department. The impervious surfaces were calculated by direct measurement, proven to be the most accurate method for measuring impervious cover (Cappiella et al., 2001). According to this method, every segment of impervious surface (i.e. roads, driveways, houses, etc.) was measured from aerial photographs with the ArcView® software. Impervious surfaces were defined for this study as any surfaces that are almost completely impervious to water including concrete or other types of pavements or water resistant material. Lawns or other grassy areas that may not be completely pervious are considered pervious for convenience. GIS soil maps were also obtained in order to detect any significant differences in soil

Table 1. Characteristics of each watershed estimated from GIS data.

	Watershed A	Watershed B	wA/wB
Area (km^2)	1.87	0.41	4.6
Impervious Cover (km^2)	0.92	0.07	13.14
% Impervious Cover	49.2	17.1	
Watershed Volume (km^3)	0.046	0.0058	7.93

types between the two watersheds. The different types of soils present in each watershed and their characteristics are summarized in Table 2. In general the soils in both watersheds were poorly drained, contained low organic matter, and were highly acidic. Their sandy nature is responsible for their relatively high permeability and low available water capacity where their acidic nature may enhance weathering of silicate minerals. The low available water capacity associated with the high permeability of the soils may reduce the ability of the watersheds to retain water.

Whereas the amount of surface runoff produced in a watershed depends on the surface area of the basin and its runoff coefficient, the amount of groundwater responsible for baseflow is governed by the specific yield of the aquifer, which depends on the volume of the aquifer that can retain water. Even though wA has an area 4.6 times larger than wB its volume is 7.93 times bigger. Since wA is larger, the flow of stream A (sA) is higher during rainfall or baseflow conditions than stream B (sB). Stream A exhibits characteristics of a stream seriously impacted by impervious cover. The channel is enlarged from extensive erosion and the substrate is fine, loose sand. Stream B is in better health with more variable substrate, more woody debris in the stream channel and a more defined pool/riffle structure.

Sample collection and analysis

Streamflow was measured using a constant dye tracer release method throughout each sampling event. Sampling station and dye injection site locations are shown in Figure 3. Low concentrations (~1,920,000 ppb) of fluorescent red

Table 2. Soil types present in each watershed and their characteristics (USDA, 1986).

Soil type	% Watershed area		Soil characteristics
	wA	wB	
Baymeade fine sand	32.56	28.50	Well drained, low organic matter, moderate permeability, slightly to strongly acidic
Kureb sand	5.43	30.68	Excessively drained, very low organic matter, rapid permeability, low available water capacity, neutral to acidic
Leon sand	19.88	0	Poorly drained, very low organic matter, rapid permeability, low available water capacity, strongly acidic
Kureb urban land Complex	0	4.68	Impacted soil beyond classification mixed with Kureb sand, very low available water capacity, rapid permiability
Lynn Haven fine sand	3.60	5.25	Poorly drained, low organic matter, rapid permeability, low available water capacity, strongly acidic
Murville fine sand	26.72	0.02	Very poorly drained, low organic matter, rapid permeability, low available water capacity, strongly acidic
Onslow loamy fine sand	0	3.50	Moderately well drained, low organic matter, moderate permeability, medium available water capacity, strongly acidic
Rimini sand	0.46	0	Excessively drained soil, very low organic matter, moderate permeability, very low available water capacity, strongly acidic.
Seagate fine sand	8.92	27.35	Poorly drained soil, low organic matter, low available water capacity, medium to very strongly acidic
Urban land	2.39	0	Unrecognizable soil series due to urbanization impact

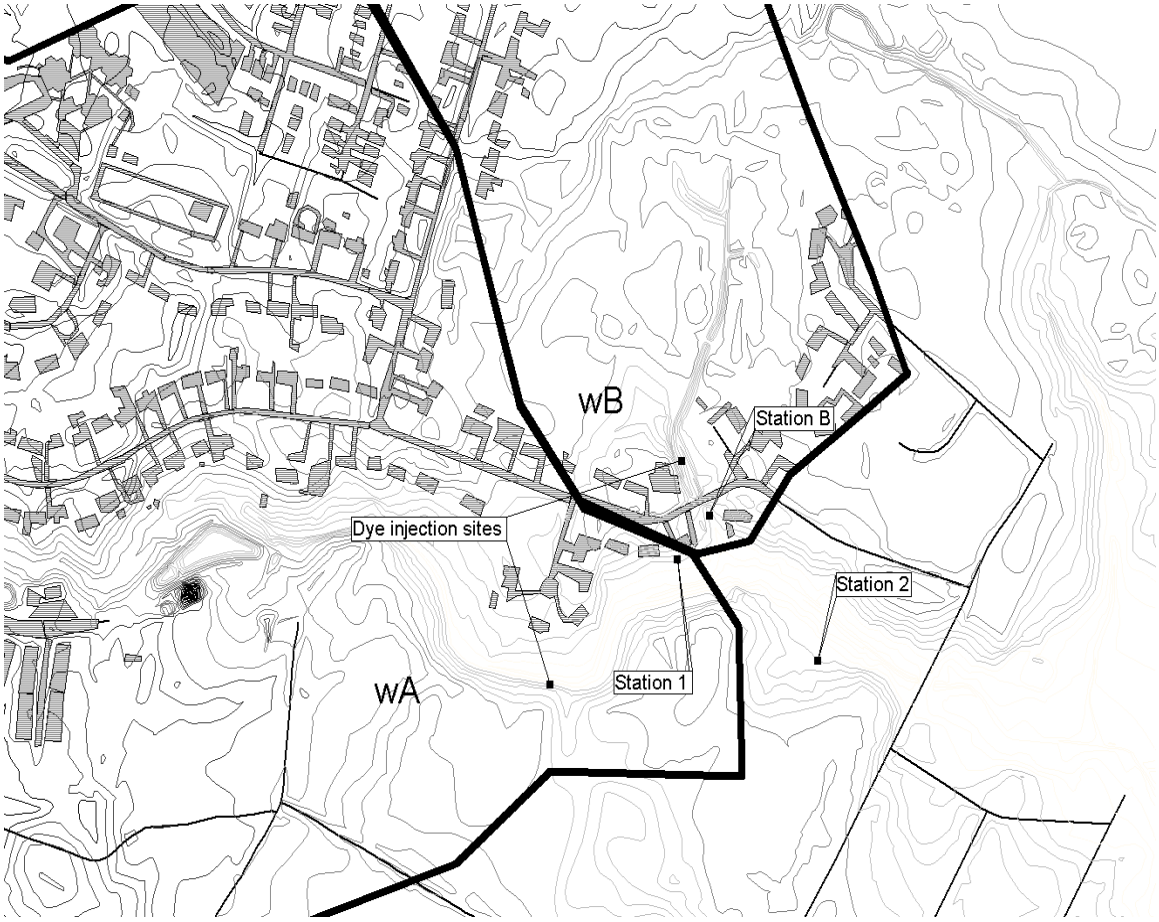

Figure 3. Map showing the sampling and dye injection sites close to the convergence point of the two streams between stations 1 and 2.

rhodamine WT dye tracer were released into sA, about 400m upstream from station 1 with the help of a field peristaltic pump throughout the sampling event at a rate of about 10-14 mL/min. The dye tracer method was chosen because it allowed, without constant attention, continuous measurements of streamflow over a desirable time period. At each sampling station an ISCO® 2900 automated sampler was programmed to collect a total of 24 discrete 100mL water samples from the stream at 45-minute intervals. The 45-minute interval was short enough to capture the rapid changes of streamflow during a rain event, but adequately long for the total sampling time (17.25 hours) to bracket a potential storm event. The samples collected were kept cool until they were transferred to the laboratory and analyzed for dissolved silica using the blue molybdate colorimetric method described by Parsons et al. (1984). The same samples were also analyzed for rhodamine WT concentration using a Turner Designs® laboratory fluorometer that can measure rhodamine concentrations as low as 1 ppt. In order to ensure accuracy and confidence in the fluorescence measurements the rhodamine concentration released was adjusted so that the concentrations in the stream were within 5-50 ppb range. The concentration of rhodamine in the various samples was inversely proportional to stream flow, which was calculated using the following equation:

$$Q = \frac{qC}{c}$$

where Q is the streamflow being measured, q is the dye injection rate, C is the concentration of the injected dye and c is the concentration of dye measured in each water sample collected. Since the dye injection rate was expected to decrease as the hydrostatic pressure in the dye reservoir decreased, the injection rate was measured at the beginning and at the end of the experiment using a 10 mL graduated

cylinder. Using the regression line plotted from the two injection rates measured, the actual injection rate at the time of each sample collection was calculated.

In order to simultaneously monitor both streams during the same rain event using only one dye release mechanism, the following sampling scheme was initially used. The dye release took place at a point 400m upstream from the site where the two streams meet on stream A (Figure 3). The distance was long enough to allow adequate mixing of the dye with the water column. Station 1 was located about 20 meters upstream from the meeting point of the two streams on sA while station 2 was about 100 meters downstream from the meeting point allowing enough distance for the two water bodies to mix. Adequate mixing of the two water bodies as well as dye mixing at each station were tested by collecting water samples along the cross-section of the stream at station 2 and analyzing them for rhodamine WT. Concentrations were uniform along the cross section of the channel. Each sampling site was equipped with a Solinist® levelloger LT capable of measuring water level and temperature at a programmed frequency. The water level data collected provided useful information on how each stream behaved during a rain event. The loggers measured relative water level as well as water temperature at a 5-minute frequency.

The DSi discharge at the time a sample was taken by the automated sampler was the product of DSi concentration of the sample times the water flow determined from the dye concentration:

$$(\text{DSi discharge}) = ([\text{DSi}] \times \text{streamflow})$$

Using the following equation the DSi discharge of sB was then calculated after DSi discharge was measured at station 1 and 2:

(DSi discharge Stream B) =

(DSi discharge at station 2) – (DSi discharge at station 1)

This relationship is based on the assumption that any groundwater or runoff inputs between the meeting point of the two streams and station 2 are insignificant. If inputs were indeed significant, the flow calculated for stream B would be overestimated. This assumption was tested with in-situ flow measurements. Streamflow was estimated using a current meter to measure water velocity and by measuring the cross-sectional area of the stream at the point of interest. Streamflow just downstream from the point of convergence of the two streams was measured as well at station 2. The streamflow difference between the two points was 0.06 m^3/min.

After a number of experiments, it became apparent that releasing the dye tracer only in sA and estimating the streamflow of sB by subtraction as described above, even though it gave representative DSi discharge estimates for both streams, could not estimate with confidence the actual DSi concentration in sB. If sB discharged higher DSi concentration water than sA, because the streamflow of sB is so much smaller than sA, the DSi concentration increase at station 2 may not have been detectable. Similar concentration of DSi at the two stations should not suggest that both streams discharged the same DSi concentration waters. Since accurate DSi concentration values for both streams were believed to be important for this project, a different sampling scheme was designed.

Instead of the peristaltic pump for the dye injection, a medical I.V. tube was attached to the 20 L reservoir that was elevated above the stream with a line attached to a tree. The I.V. tube was equipped with a flow regulator and a drip chamber allowing

precise and accurate injection rates. Because of the low cost of the new dye injection unit compared to the peristaltic pump unit used earlier, an additional unit was constructed and deployed at sB in order to obtain independent flow measurements in both streams. Under this new deployment scheme, station 2 was abandoned and a new sampling site was created on sB, about 20 m upstream from where the two streams meet. Since the range of flow in sB was considerably lower than sA, the concentration of the injected dye was reduced to 800,000 ppb. The dye was injected 80 meters above the sampling site on sB. Even though the distance allowed for mixing was considerably shorter than the one in sA, it was sufficient since mixing was enhanced by the pool/rifle structure of the stream channel as well as the woody debris and rocks present.

Well samples were collected from a shallow well (~4m) located in wA (Figure 2) and a deeper well (~23m) to determine the groundwater DSi concentration of the shallow and deep aquifers. The wells were purged prior to sample collection. Samples were kept cool (~4° C) but never allowed to freeze since freezing was found to polymerize DSi, a form undetectable by the analytical method used.

The greatest advantage of the close proximity of the watersheds was the ability to observe the two streams during the same rain event. Since the sub-watersheds were adjacent to each other it was reasonably safe to assume that rainfall patterns (intensity, duration and volume) were relatively uniform over the entire study area. A digital rain gage installed between the two sampling sites monitored the rainfall intensity and total height throughout each sampling event.

Seventeen experiments were performed, however, only nine successfully produced useful data. Since sampling often took place during adverse weather

conditions, instrument malfunction was not a rare phenomenon. Five events were sampled during baseflow conditions and 4 during rain events. DSi concentrations during baseflow events allowed the establishment of a baseline for each stream. These baseline concentrations were statistically compared between the streams using a one-way ANOVA. All ANOVA analyses were performed using SAS v. 8.01 software. Streamflow during non-rain events was also compared between streams. Since streamflow during non-rain events was a function of the amount of water available in the aquifer at the time of the event, it was expected to vary significantly between events. The same variability was expected for the rest of the parameters that were functions of streamflow including DSi discharge. In order to statistically compare variability between streams while ignoring any variability between events, the events were used as a blocking factor in a 2-way ANOVA. The DSi discharge/km^3 and streamflow/ km^3 of watershed were calculated by dividing DSi discharge and streamflow respectively by the watershed volume. Streamflow/km^2 and DSi discharge/km^2 were calculated in the same manner by dividing streamflow and DSi discharge by watershed area. DSi discharge/km^3, streamflow/km^3, DSi discharge/km^2 and Streamflow/km^2 were statistically compared between streams using a two-way ANOVA. During rain events, the response of DSi concentration and discharge to the varying streamflow was observed. Total DSi and water discharged from each stream over the 17.25-hour events were calculated. A regression analysis was performed to test correlation between rainfall and total DSi as well as total water discharged. Regression lines were compared between streams using analysis of covariance.

In order to reduce variations between watersheds that could not be controlled (i.e., baseflow, background DSi concentration), a new comparison was concentrated on the part of the storm hydrograph representing only the stormwater, the excess water discharged due to rainfall (see Figure 4). If from the total water discharge, represented by the total area of the hydrograph, beseflow is subtracted then the remaining area represents the water discharged as surface runoff along with the water discharged as interflow, also known as subsurface stormflow (Leopold, 1978). Interflow is defined as the additional baseflow discharged due to the rain event since baseflow too can increase during rain. In order to separate the hydrograph into the 3 sections, the following method was used. The baseflow volume was calculated by averaging the streamflow values obtained from the samples collected before rainfall began. The average was then multiplied by the total number of minutes (1035) of the sampling event. The baseflow volume was subtracted from the total volume of streamflow calculated through integration. In order to separate the stormwater part of the hydrograph into runoff and interflow the DSi concentration of the stormwater had to be determined first. The plot of the DSi discharge over time was also separated into 3 sections in the same manner as the hydrograph. The amount of DSi (moles) contained in the stormwater part of the hydrograph divided by the volume of stormwater gave the total concentration of the stormwater. Assuming that the DSI concentration of the interflow was equal to the baseflow DSi concentration the following equation was then used to calculate the volume of interflow:

$$V_I = \frac{V_S \times C_S}{C_B}$$

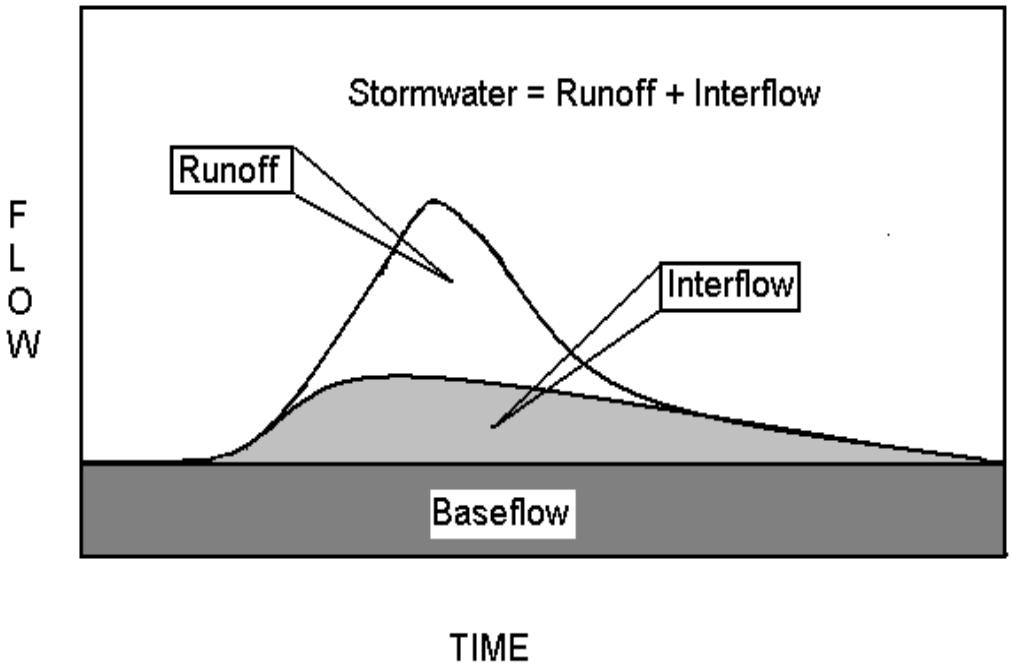

Figure 4. Streamflow hydrograph separated into the three sections.

Where V_I is the volume of Interflow, V_S the stormwater volume, C_S is the stormwater DSi concentration and C_B is the DSi concentration of the baseflow determined from pre-rain samples. The volume of runoff, assumed to contain 0 μM DSi, was calculated by subtracting the baseflow volume from the total stormwater volume. The amount of runoff and interflow generated from each watershed during each rain event was calculated. Runoff and interflow per km^2 and km^3 were also calculated.

Since the number of rainfall events sampled was limited, a different method was used to predict the response of each watershed over a larger time period encompassing a larger spectrum of precipitation. The Soil Conservation Service's (SCS) curve number (CN) method allowed the calculation of runoff generation by each watershed (USDA, 1986). Curve numbers were estimated based on soil hydrologic properties and land use data of each watershed.

According to the CN method, runoff height is calculated using the following equation:

$$Q = \frac{(P - 0.2S)^2}{(P + 0.8S)}$$

Where Q was the height of runoff (cm), P was the rainfall and S was the potential maximum retention after runoff begins (cm) estimated by:

$$S = \frac{1000}{CN} - 10 .$$

Soil and land use GIS data were used for the determination of curve numbers for each watershed. Curve numbers were functions of several parameters including area of impervious surface, area of pervious surface, type and condition of vegetation and soil types in each watershed. Using daily rainfall data provided by the National Climatic Data Center (NCDC) for two consecutive years (2001-2002), CN curves were plotted for each

watershed (Figure 5). These curves represented the relationship between rainfall and runoff production and allowed the estimation of the x intercept, which represented the minimum amount of rain capable of producing runoff. The total amount of runoff and DSi discharge throughout the 2-year period were estimated for each watershed. The total DSi discharged by each watershed was calculated by subtracting the total runoff produced from the total volume of rainfall collected by each watershed and multiplying the resulting volume by the average baseflow DSi concentration to give the total amount of DSi discharged in moles. The results were then normalized by watershed area and volume.

RESULTS

Baseflow

Baseflow parameter averages and standard deviations are summarized in Table 3. Stream A had an average DSi concentration of 72.43 μM (n=120, std dev= 4.380), whereas sB had an average of 67.60 μM (n=55, std dev=2.074). One-way ANOVA, showed a significant difference ($F=60.39$, $p<0.0001$ $df=1, 173$) between the baseflow DSi concentrations of the two streams.

Because streamflow was expected to vary significantly between events, a 2-way ANOVA was chosen for the comparison of parameters dependent on streamflow. In the two-way ANOVA, the streams and events were the two possible sources of variation. Even though differences among events were not of interest, by including the event as a blocking factor in the ANOVA, any variations among events were corrected, giving more confidence to the test for the main effect. Interaction between events and streams was not of interest and wasn't included in the ANOVA test. Streamflow was higher during

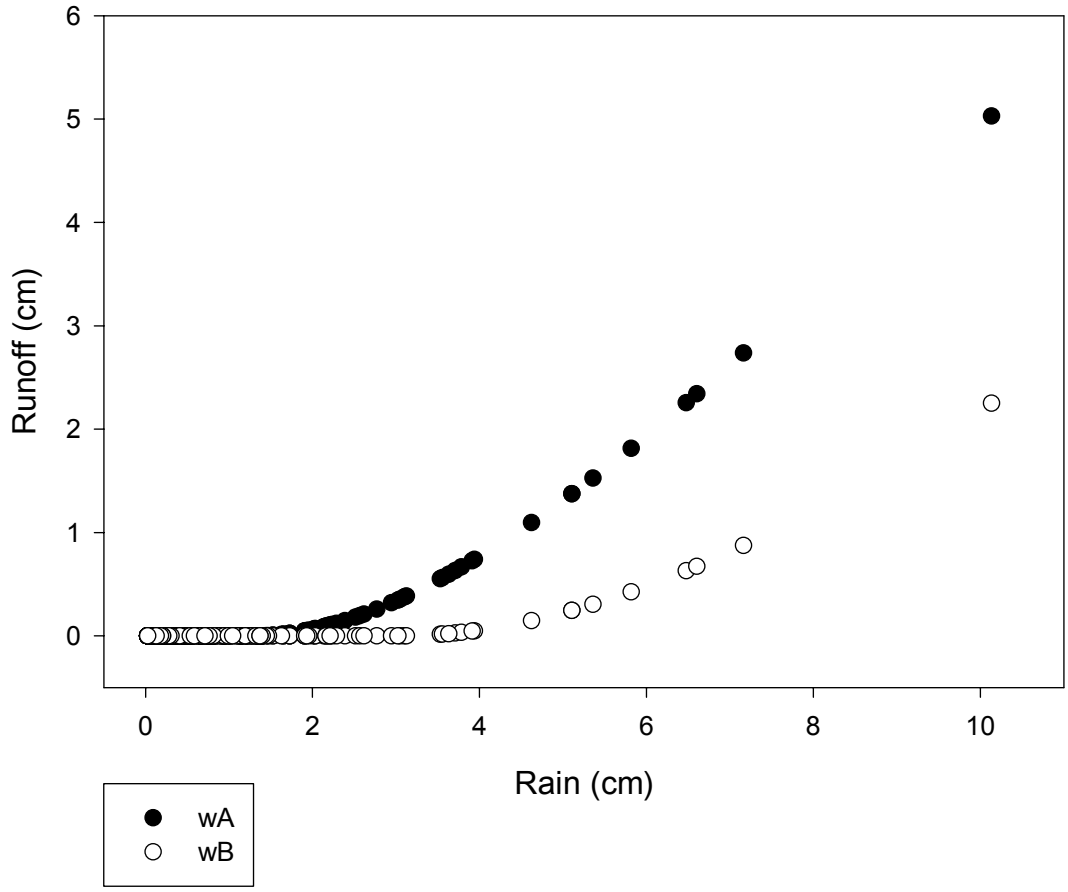

Figure 5. CN curves for each watershed calculated using 2001-2002 daily rainfall data. CN curves represent the relationship between rainfall and runoff production on a watershed.

Table 3. Means and ANOVA results for the various parameters calculated from non-rain event data.

Parameter	Mean Std. Dev.		F Value	P value	d.f.
	sA	sB			
[DSi] (μM)	72.43 4.380	67.60 2.074	60.93	<0.0001	1 173
Streamflow (m^3/min)	2.877 0.617	0.351 0.246	2440.20	<0.0001	1 234
DSi Discharge (moles/min)	0.241 0.076	0.024 0.019	1987.32	<0.0001	1 234
Streamflow/Volume m^3/min·km^3	72.32 22.07	60.71 42.93	17.68	<0.0001	1 234
Streamflow/Area m^3/min·km^2	1.75 0.57	0.85 0.62	415.2	<0.0001	1 234
DSi Discharge/Volume (moles/min·km^3)	5.255 1.670	4.168 3.310	20.72	<0.0001	1 234
DSi Discharge/Area (moles/min·km^2)	0.129 0.041	0.052 0.051	445.6	<0.0001	1 234

non-rain events in sA (mean=2.880m^3/min, std dev=0.619) than in sB (mean= 0.352m^3/min, std dev=0.249) according to the 2-way ANOVA [Treatment: ($F=2440.20$, $p<0.0001$, df=1, 234), Block ($F=25.94$, $p<0.0001$, df=4, 234)]. DSi discharge was significantly higher in sA (mean=0.241 moles/min, std dev=0.076) than in sB (mean=0.024 moles/min, std dev=0.019) according to the 2-way ANOVA performed [(Treatment ($F=1987.32$, $p<0.0001$, df=1, 234), Block ($F=72.12$, $p<0.0001$, df=4, 234)].

Streamflow per km^3 of watershed was also calculated and compared between watersheds during the several non-rain events and found to be significantly different [Treatment ($F= 17.68$, $p<0.0001$, df=1,234), Block ($F=93.07$, $p<0.001$, df=4, 234)]. Stream A had an average discharge of 72.32m^3/min·km^3 (std dev=22.07) while sB had an average of 60.71m^3/min·km^3. DSi discharge rate per km^3 of watershed was higher for sA (mean=5.255 moles/min·km^3, std dev=1.670) than for sB (mean=4.16 moles/min·km^3, std dev=3.310). A 2-way ANOVA showed a significant treatment effect [Treatment ($F=20.72$, $p<0.0001$, df=1, 234), Block ($F=61.09$, $p<0.001$, df=4, 234)]. Streamflow per km^2 between watersheds during the several non-rain events was also significantly different [Treatment ($F= 415.17$, $p<0.0001$, df=1,234), Block ($F=121.59$, $p<0.001$, df=4, 234)]. Stream A had an average streamflow of 1.75m^3/min·km^2 (std dev=0.57) while sB had an average of 0.85m^3/min·km^2 (std dev=0.62). DSi discharge rate per km^2 of watershed was higher for sA (mean=0.129 moles/min·km^2, std dev=0.041) than for sB (mean=0.052 moles/min·km^2, std dev=0.051). A 2-way ANOVA showed a significant treatment effect [Treatment ($F=445.60$, $p<0.0001$, df=1, 234), Block ($F=103.02$, $p<0.001$, df=4, 234)].

Samples collected from the shallow well in wA gave a mean concentration of 66.3μM (std dev=4.8, n=6), which was similar to baseflow concentrations found in both streams (Figure 6). Samples collected from the deeper well, a few meters away from the shallow well, gave higher DSi concentrations (136.7μM (std dev=30.93, n=6).

Rain events

Plots were created for each event that showed the response of several parameters to the increasing streamflow during a rain event. Representative examples are shown in Figures 7, 8, and 9. Only two rain events are presented since only during those two events DSi concentration samples were collected directly from sB. A significant decrease of DSi concentration was observed with increasing streamflow in sA whereas DSi concentration in sB remained constant throughout the rain event. During the lighter rain event that took place on June 4, 2003 (0.35 cm), the streamflow of sA experienced a 64% flow increase whereas the flow of sB did not change at all. DSi concentration dropped by 18% in sA whereas sB did not change significantly. During the heavier rain event in July 2003 (2.33 cm), the streamflow of sA increased by 198% where as the streamflow of sB increased by 30%. Concentration of DSi in sA decreased by 47% but in sB no significant change was observed. The DSi discharge for sA during the same event increased by 108% and in sB it increased by 27%.
For each of the four rain events, total water volume (m^3) and total DSi (moles) discharged over the 17.25-hour sampling events were calculated. Results are summarized in Table 4. Total water and DSi discharge were higher in sA than sB. Total water and DSi discharge per unit volume and area of watershed were also

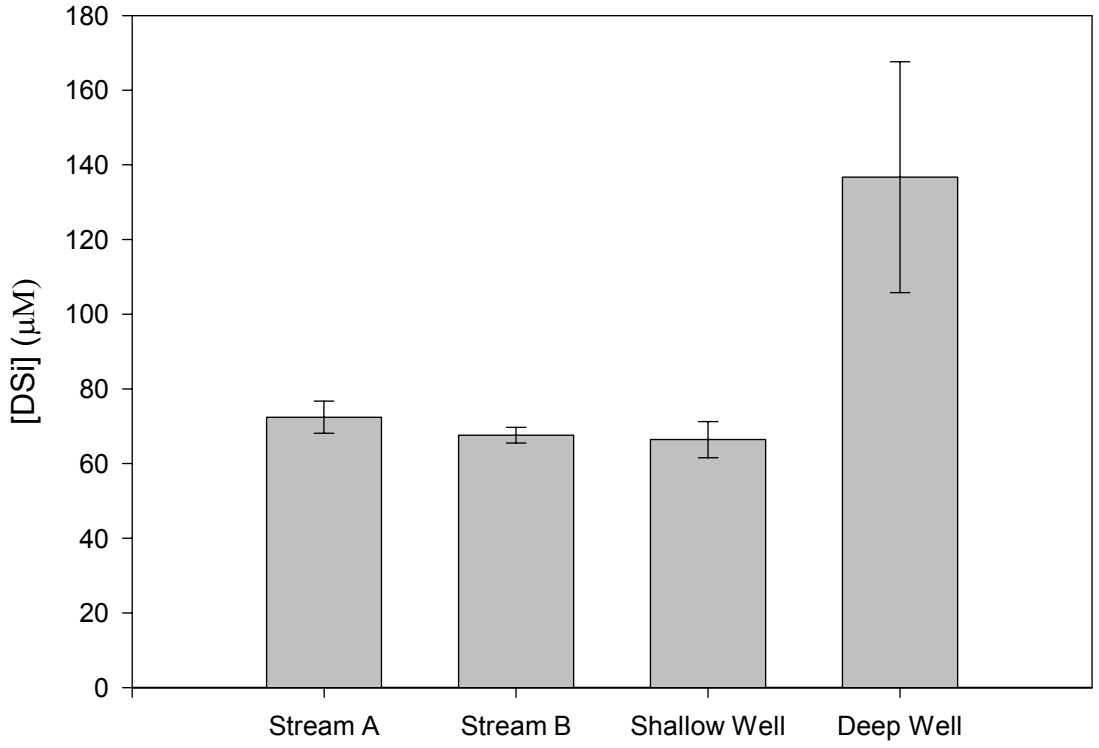

Figure 6. DSi concentrations of the two streams and groundwater wells during non-rain events. (Stream A: mean=72.4μM, std dev=4.38, n=120. Stream B: mean=67.6μM, std dev=2.07, n=55. Shallow well: mean=66.3μM, std dev=4.80, n=6. Deep well: mean=136.7μM, std dev=30.9, n=6)

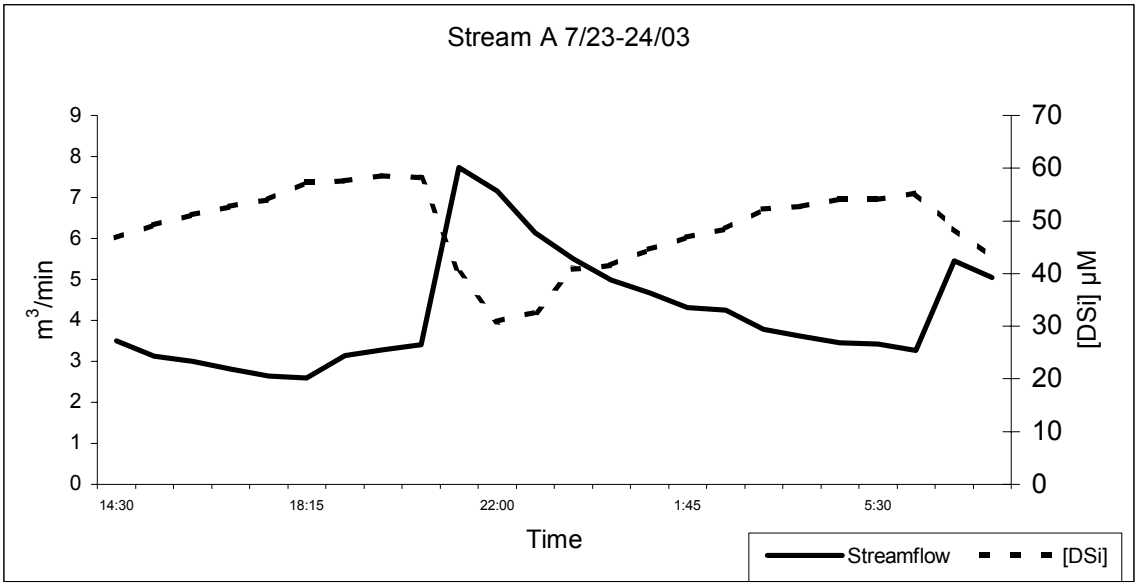

a.

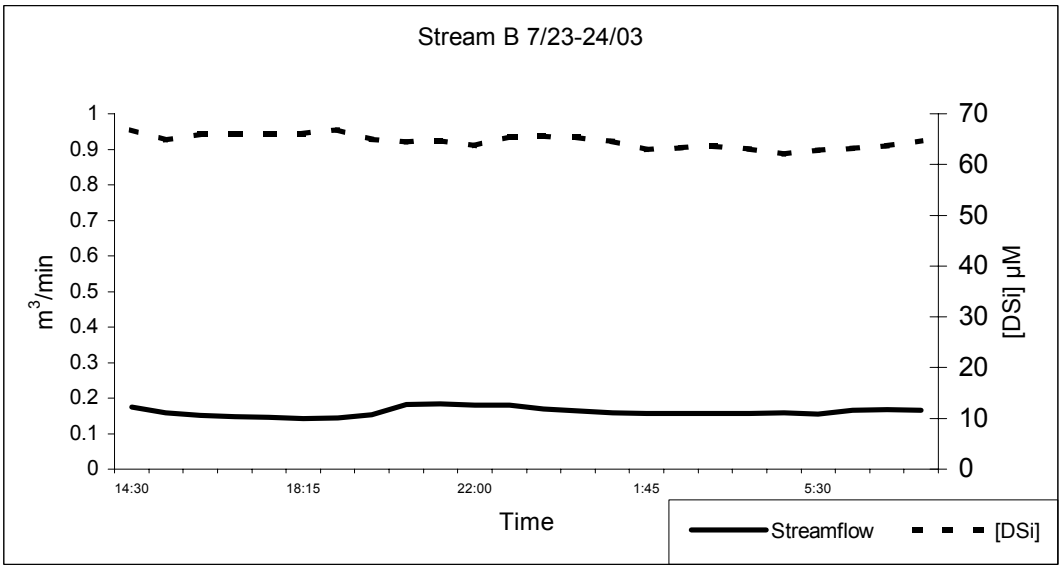

b.

Figure 7. DSi concentration response to streamflow increase during a rain event (July 23-24, 2003) in the two streams (Rain=2.34cm). a.) Stream A b.) Stream B

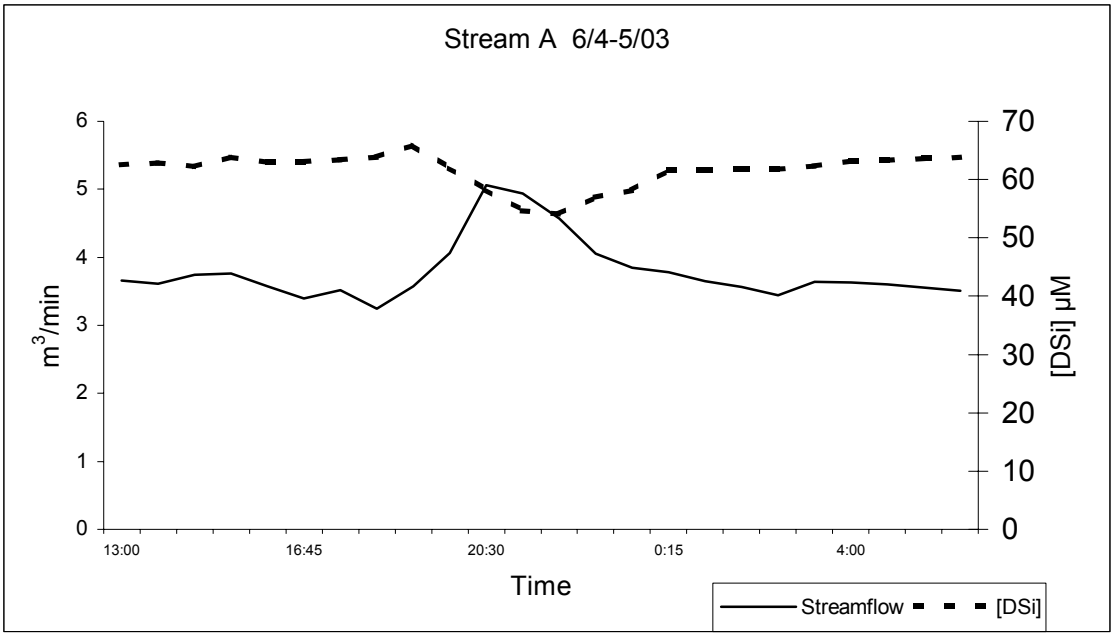

a.

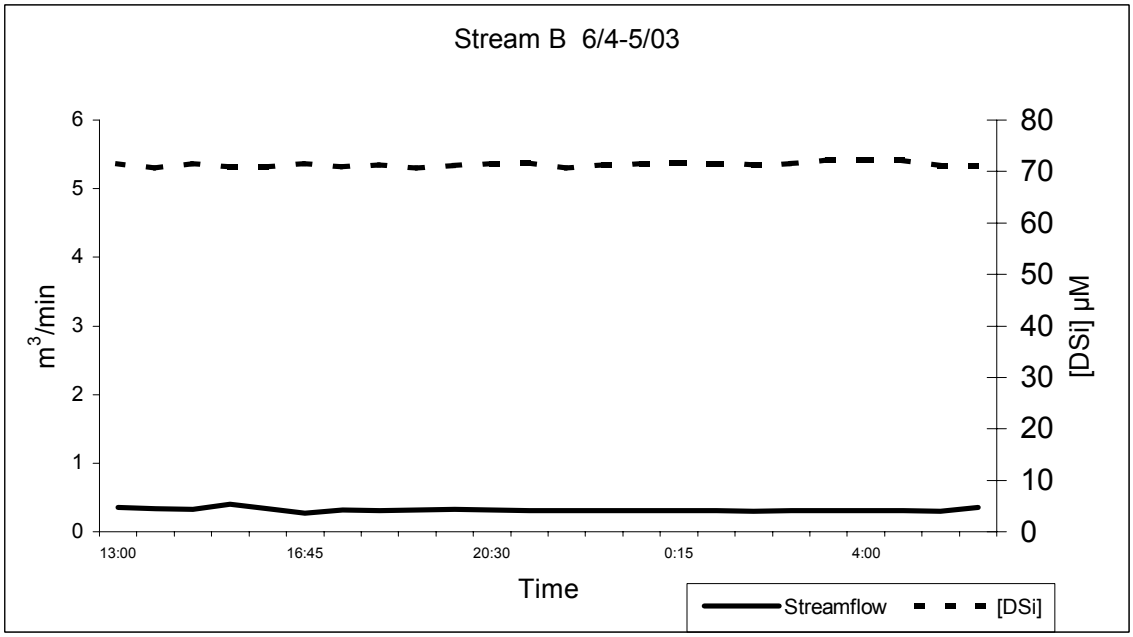

b.

Figure 8. DSi concentration response to streamflow increase during a rain event (June 4-5, 2003) in the two streams (Rain=0.35cm). a.) Stream A b.) Stream B

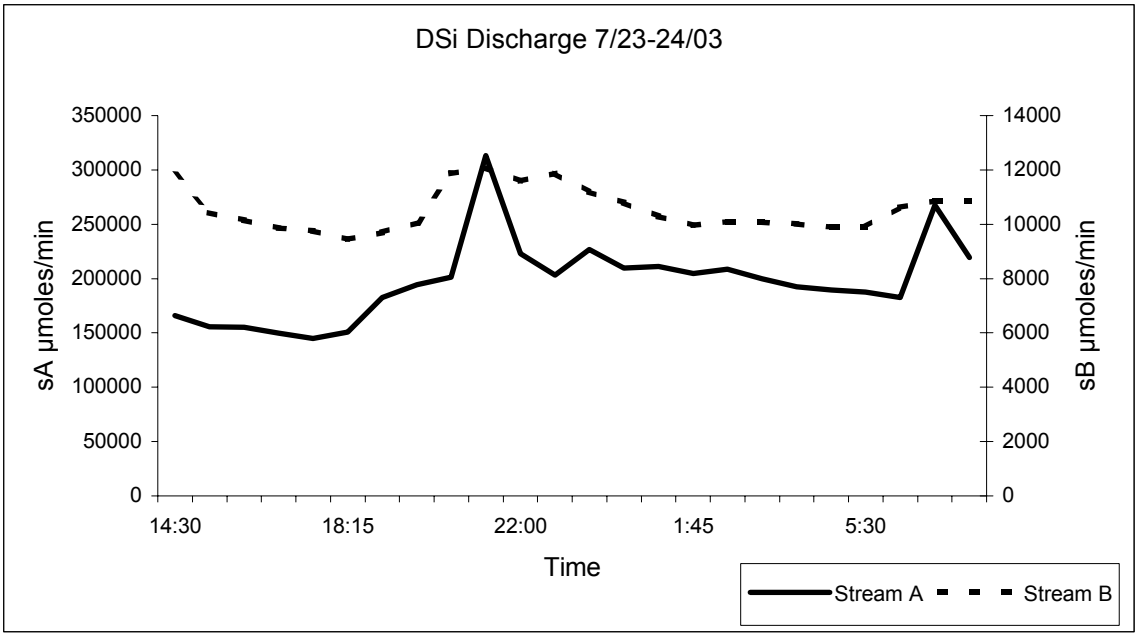

a.

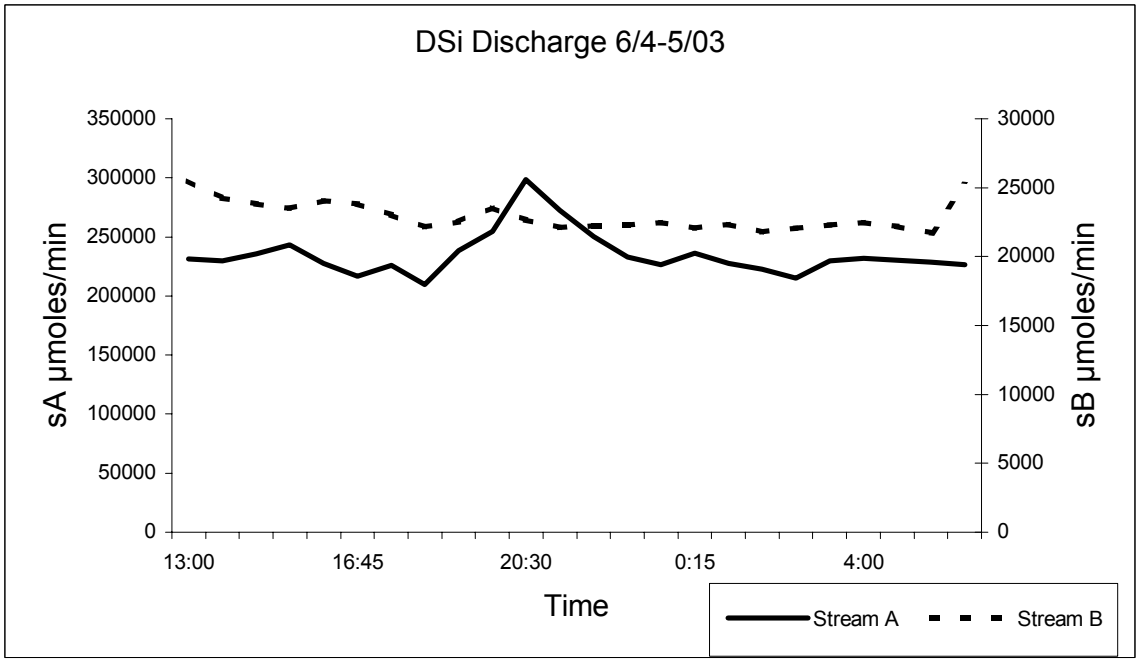

b.

Figure 9. DSi discharge for each stream during two different rain events. a.) April 23-24, 2003 (Rain=2.34cm). b.) June 4-5, 2003 (Rain=0.35).

Table 4. Total water and DSi discharge over each rain event with per unit watershed calculations incorporated.

Event date		4/25/03	5/22/03	6/4/03	7/23/03
Rainfall (cm)		4.90	11.8	0.34	2.34
Total Water discharge (m^3)	sA	13,200	21,240	3,978	4,369
	sB	1,712	7,385	331	169
Total DSi discharge (moles)	sA	358.5	392.3	243.6	204.6
	sB	34.6	125.3	23.6	10.6
Total Water discharged by 1 km^3 of watershed (m^3)	sA	287,000	461,700	86,490	94,990
	sB	295,200	127,300	57,050	29,100
Total Water discharged by 1 km^2 of watershed (m^3)	sA	7,060	11,360	2,127	2,336
	sB	4,175	18,010	807	412
Total DSi discharged by 1 km^3 of watershed (moles)	sA	7,794	8,528	5,296	4,447
	sB	5,972	21,610	4,071	1,921
Total DSi discharged by 1 km^2 of watershed (moles)	sA	191.7	209.7	130.3	109.4
	sB	84.4	305.6	57.6	25.9

calculated by dividing the total volume of water or the DSi discharged during the sampling event by the volume or area of each watershed accordingly. The results obtained from these calculations showed that sA discharged more water and DSi per km^3 and km^2 of watershed than sB in 3 out of 4 rain events (Figure 10 and 11).

Total DSi and water discharge showed a positive correlation with rainfall height in both streams (Figure 12). Analysis of covariance showed that the slopes of the two regression lines in Figure 12 a. (sA: slope= 15.27 moles/cm, std err= 6.79, R^2=0.716; sB: slope= 9.91 moles/cm, std err= 5.96, R^2=0.89) were not significantly different (F=0.549, p=0.50, df=1, 4) suggesting that DSi discharge increased with rain in each stream in a similar fashion. In Figure 12 b. the slope of sA is significantly greater (F=15.58, p<0.025, df=1, 4) than sB (sA: slope=1670.86m^3/cm, std err=272.720, R^2=0.95; sB: slope =663.71m^3/cm, std err=110.43, R^2 =0.94) suggesting that wA can produce more runoff faster than wB. The data collected during each rain event were corrected for baseflow in order to eliminate effects that could not be controlled and to study solely the effect rainfall had on each stream. This was done by separating the streamflow and DSi discharge hydrographs into 3 sections (Figure 4). This method allowed me to calculate how much runoff ([DSi]=0) and how much interflow were discharged by each stream during each rain event. Results obtained using this approach are summarized in Table 5.

As one would expect, sA discharged more runoff as well as interflow than sB in every rain event because of the larger area and volume wA occupied. After these two parameters were normalized by area and volume of watershed, however, sA discharged more runoff per km^2 and km^3 of watershed than sB in only 3 events out of 4.

Figure 10.

a.) Relationship between total DSi discharged per km^3 of watershed and total precipitation for each rain event.

b.) Relationship between total water discharged and total precipitation for each rain event

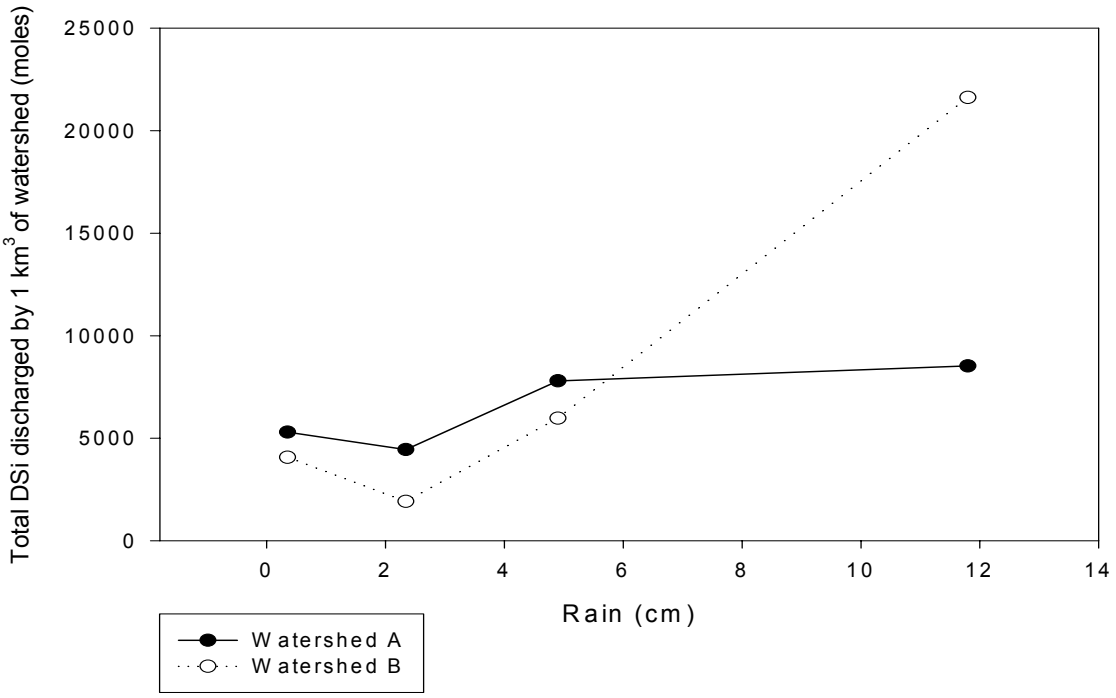
Total DSi discharged by 1 km3 of watershed (moles)
25000
20000
15000
10000
5000
0
0
2
4
6
8
10
12
14
Rain (cm)
Watershed A
Watershed B

a.

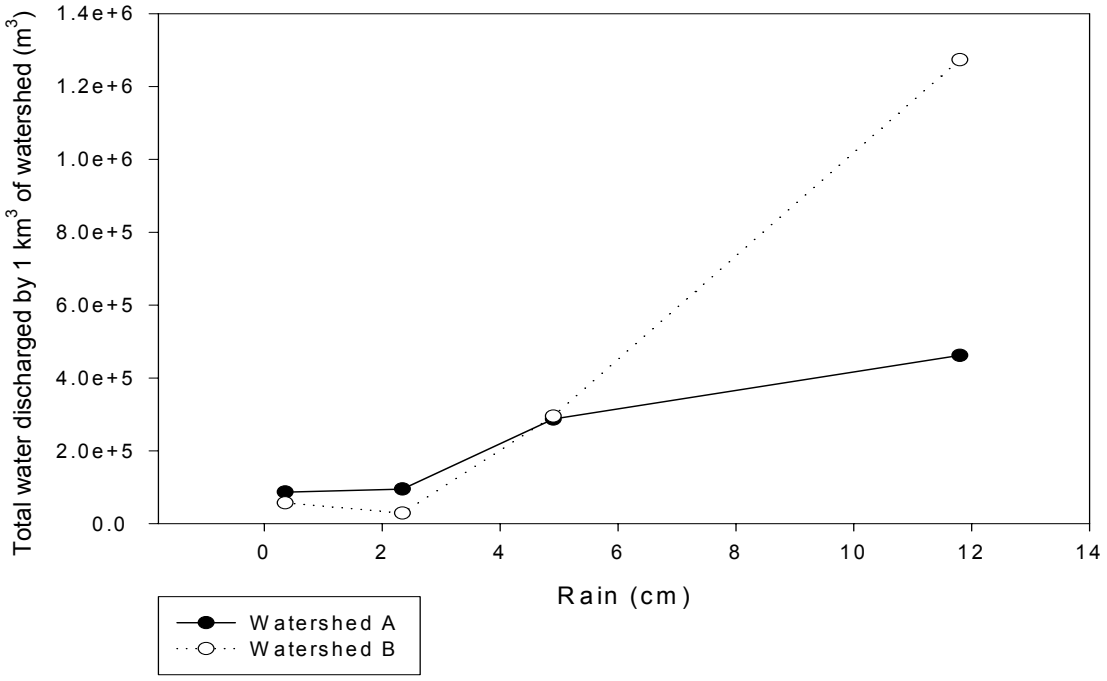
Total water discharged by 1 km3 of watershed (m3)
1.4e+6
1.2e+6
1.0e+6
8.0e+5
6.0e+5
4.0e+5
2.0e+5
0.0
0
2
4
6
8
10
12
14
Rain (cm)
Watershed A
Watershed B

b.

Figure 11.

a.) Relationship between total DSi discharged per km^2 of watershed and total precipitation for each rain event.

b.) Relationship between total water discharged and total precipitation for each rain event

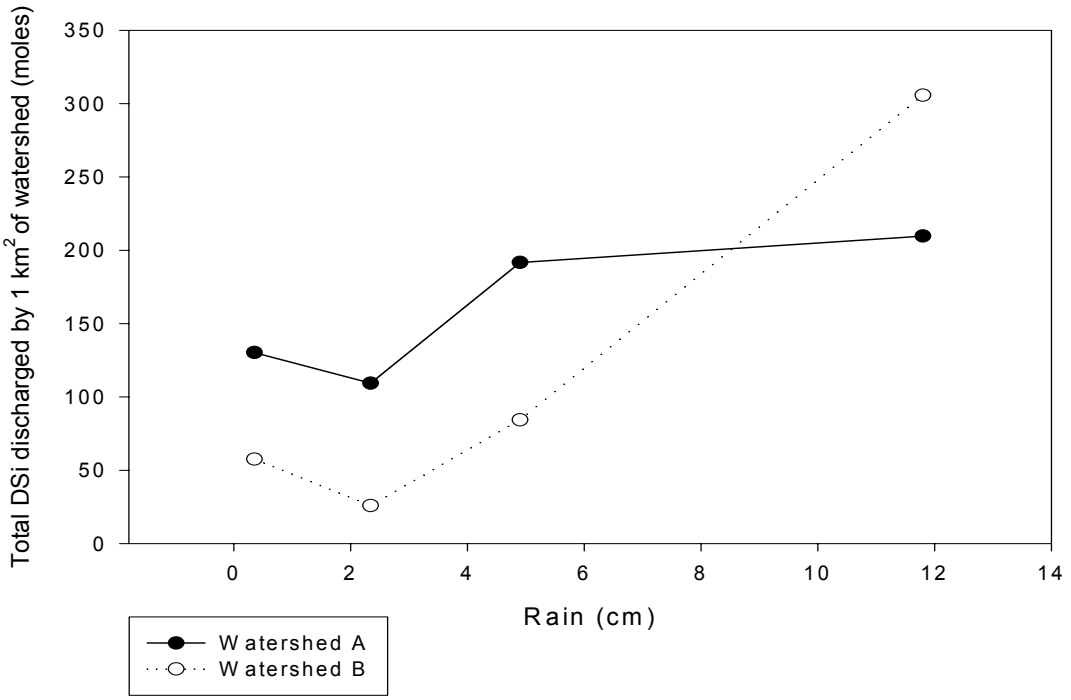
Total DSi discharged by 1 km2 of watershed (moles)
350
300
250
200
150
100
50
0
0
2
4
6
8
10
12
14
Rain (cm)
Watershed A
Watershed B

a.

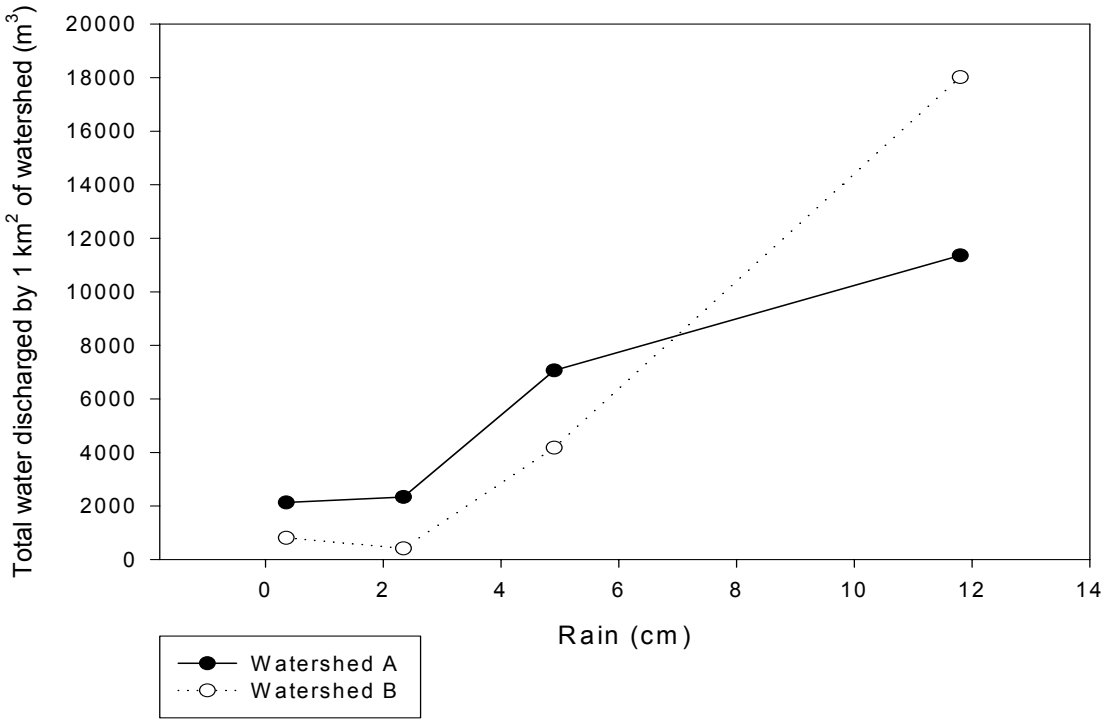
Total water discharged by 1 km2 of watershed (m3)
20000
18000
16000
14000
12000
10000
8000
6000
4000
2000
0
0
2
4
6
8
10
12
14
Rain (cm)
Watershed A
Watershed B

b.

Figure 12.

a.) Relationship between total DSi discharged and total precipitation for each rain event.

b.) Relation between total water discharged and total precipitation for each rain event.

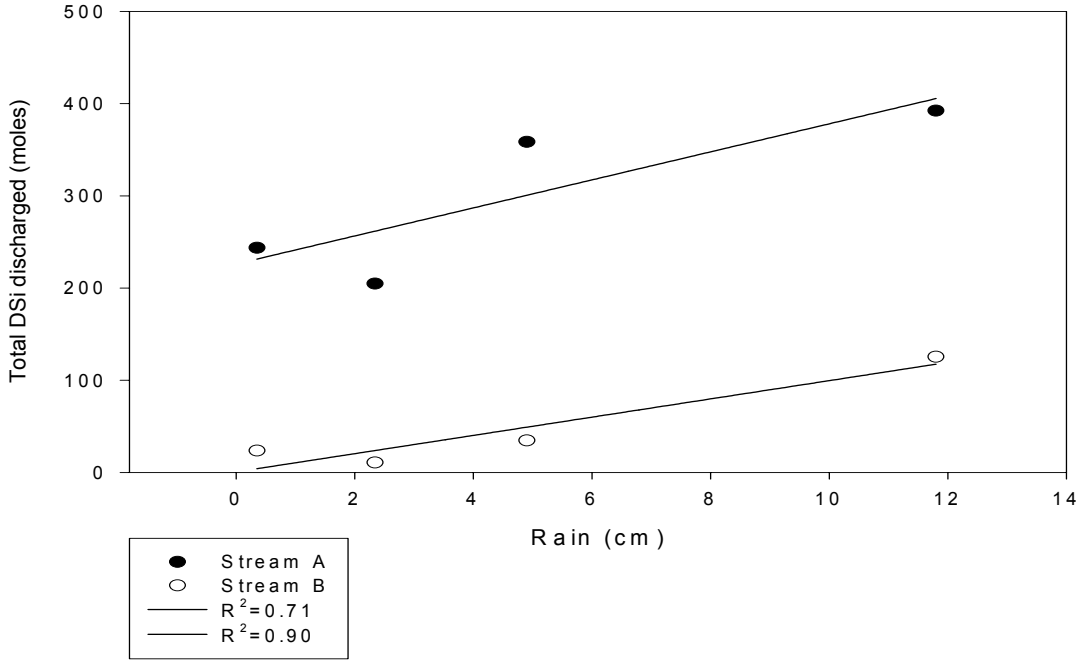
Total DSi discharged (moles)
500
400
300
200
100
0
0
2
4
6
8
10
12
14
Rain (cm)
Stream A
Stream B
R2=0.71
R2=0.90

a.

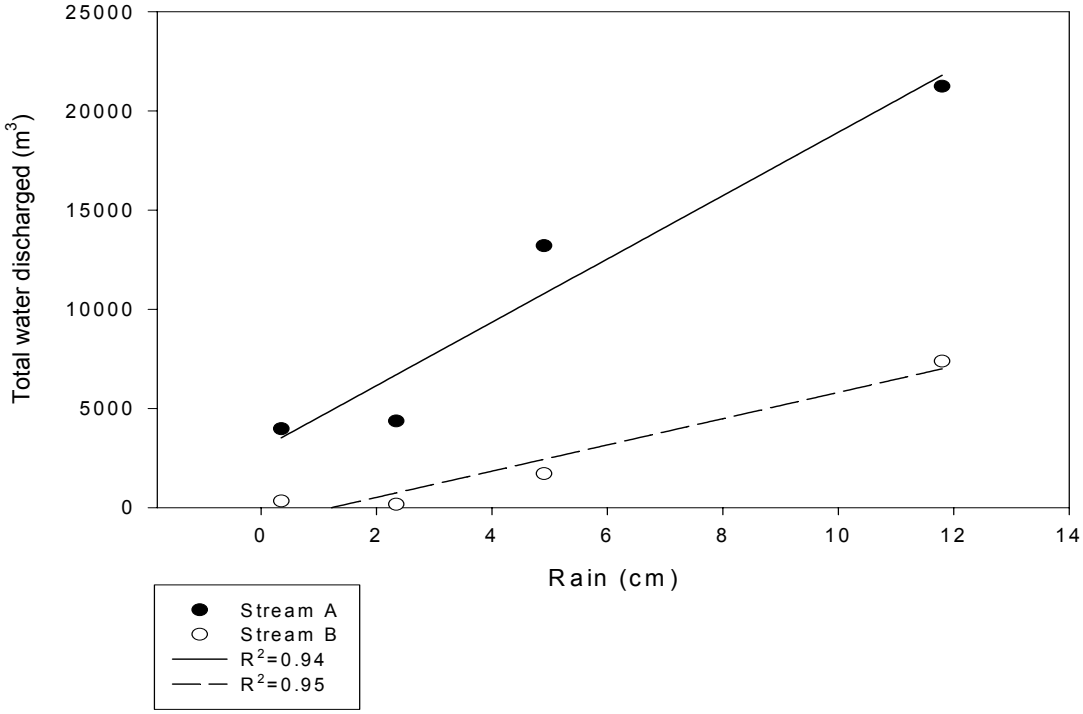
Total water discharged (m3)
25000
20000
15000
10000
5000
0
0
2
4
6
8
10
12
14
Rain (cm)
Stream A
Stream B
R2=0.94
R2=0.95

b.

Table 5. Stormwater discharge data for the two streams with baseflow discharge subtracted.

Event date		4/25/03	5/22/03	6/4/03	7/23/03
Rainfall(cm)		4.90	11.8	0.34	2.34
Runoff (m^3)	sA	8,488	14,170	112	407
	sB	1,231	5,118	0	0
Interflow (m^3)	sA	932	2,705	87	877
	sB	239	1,955	0	8
Runoff/km^2	sA	4,539	7,578	60	218
	sB	3,002	12,480	0	0
Runoff/km^3	sA	184,500	308,100	2,434	4,739
	sB	212,200	882,400	0	0
Interflow/km^2	sA	498	1,447	46	469
	sB	3,002	4,768	0	20
Interflow/km^3	sA	20,260	58,800	1,891	19,070
	sB	41,330	337,200	0	1,362
Runoff/Interflow	sA	9.1	5.2	1.3	0.5
	sB	5.1	2.6	0.0	0.0
DSi (moles)	sA	71.0	150.5	5.5	45.6
	sB	17.4	108.4	0.0	0.5
DSi/km^2	sA	38.0	80.5	2.9	24.4
	sB	42.4	264.4	0.0	1.2
DSi/km^3	sA	1,543	3,271	119.1	990.2
	sB	3,000	18,690	0.0	93.1

Two times out of 4, sA discharged more interflow per km^2 and km^3 than sB as well as more DSi. It should be pointed out that for every rain event, the runoff/interflow ratio was always lower for sB. An important finding that rose from this approach is that sB did not discharge any runoff at all during the two lowest rainfall events. On June 4, 2003, in particular, when rainfall did not exceed 0.34cm the streamflow of sB was not affected at all but an increase of interflow and runoff was recorded in sA.

According to the CN method used, wA started to produce runoff when rainfall reaches 1.34cm, earlier than wB which required more than twice the amount of rainfall to produce runoff (3.05cm). The predicted amount of runoff and total DSi discharged by each watershed during the 2-year period are shown in Table 6.

DISCUSSION

Baseflow

During non-rain events both streams were mostly fed by groundwater. This was supported by the DSi concentrations of the shallow well samples collected. The well sample concentrations were very similar to baseflow concentrations in samples collected from both streams (Figure 6). On average, sA discharged higher [DSi] water than sB during baseflow. Even though the ANOVA showed that concentrations were indeed different ($F=60.39$, $p<0.0001$ $df=1, 173$) Figure 6 shows that the difference was small but most likely consistent throughout the experiments. Many factors may control the concentrations of DSi in groundwater including retention time of water in the aquifer, soil mineral content and chemical properties. It was not feasible, however, to identify all of the factors that controlled the baseflow DSi concentrations in the streams and

Table 6. Total loads discharged by each watershed during a 2-year period (2001-2002) estimated using the CN method.

	wA	wB
Total rainfall volume (m^3)	4,469,000	980,000
Total runoff (m^3)	527,200	24,640
Runoff/km^2 (m^3)	281,900	60,100
Runoff/km^3 (m^3)	11,460,000	4,248,000
Total Baseflow (m^3)	3,942,000	955,300
Baseflow/km^2 (m^3)	2,108,000	2,330,000
Baseflow/km^3 (m^3)	85,700,000	164,700,000
Total DSi (moles)	285,400	64,580
DSi/km^2 (moles)	152,600	157,500
DSi/km^3 (moles)	6,205,000	11,130,000

because the difference (4.83μM) was not large further investigation was not considered.

Not surprisingly, streamflow was higher in sA since wA was almost 8 times larger than wB. The DSi discharge per unit volume and area of watershed, however, was unexpectedly higher in sA than sB. According to the main hypothesis of this study sB, was expected to discharge more DSi as well as water per unit watershed than sA. That was expected since wA has higher percent impervious cover. Higher percent impervious cover would reduce infiltration, thus reducing the amount of water stored in the aquifer. Such conditions should lead to lower than normal baseflows as Klein (1979), Spinello and Simmons (1992) suggested through their work (see page 13). The main hypothesis was based on the assumption that the two watersheds behaved in exactly the same way. The results, however, showed clearly that the two watersheds did not behave in the same way. The fact that sB did not discharge more water or DSi per unit volume or area of watershed could be a result of many different factors that could not be predicted or measured. A watershed's water budget and cycle may include numerous variables including stormwater management practices, evapotranspiration, water use, etc. Significant water withdrawal from deeper groundwater aquifers and subsequent discharge in the watershed via irrigation etc, for example, could account for higher than expected streamflow or even DSi in either stream. Samples taken from a deeper well a few meters away from the shallow well in wA showed that DSi concentrations in deeper aquifers were significantly higher (mean=119.6μM, std dev=28.29, n=6). This volume of water, used for watering lawns, washing cars and pavements, could end up in the streams as either baseflow or runoff.

The sampling events during baseflow conditions helped establish a baseline to which changes during rain events were compared. DSi concentrations ranged between 60 μM and 80 μM but they were relatively consistent within each stream (see table 3) even though sampling events ranged from March to July. These results are a good indication that DSi concentrations of the shallow aquifer in the area remained stable for at least that part of the year. Streamflow varied within each stream between events, as expected, since streamflow depends on the amount of water stored in the aquifer at that particular day and time. Baseflow increased after a rain event and then gradually decreased until the next rain.

Rain events

During rain events, DSi discharge increased in both streams when streamflow increased. According to Figure 12 a, DSi discharge increased at a similar rate with increasing precipitation. Since wA is so much larger than wB, one would expect that total DSi discharge would increase at a much faster rate in sA than in sB. Instead the slopes were not found to significantly differ. Streamflow on the other hand increased significantly faster in sA than in sB. Since streamflow in sA increased faster with increasing rain than in sB but yet total DSi did not, it is likely that the flow increase in sA was mostly caused by low DSi concentration runoff.

As seen in Table 4, DSi discharge per unit watershed volume and area was higher in sA than in sB. It was thought that because wA would generate more runoff than wB, sB would discharge more DSi per unit watershed volume and area than sA. That, however, was the wrong approach to the issue this study was designed to

address. DSi discharge, since it is the product of DSi concentration and streamflow, should increase as long as streamflow increases faster than DSi concentration drops. For a stream like sA with such a high percent of impervious cover, streamflow increases rapidly because of the large amount of runoff generated. Even if DSi concentration drops, the increase of flow is so much higher, that there is always a net increase of DSi discharge. Further, because baseflow DSi discharge per unit watershed was already higher during baseflow it remained higher following rain events. According to Figure 10 and 11, on three out of four occasions sA discharged more water and DSi per km^3 and km^2 watershed than sB. During the most intense rain event, however, (11.8 cm) sB discharged significantly more water and DSi per km^3 or km^2 than sA. Even though it was an isolated event, it may still suggest that the behavior of the watersheds may have changed significantly beyond a certain amount of rainfall. In other words rain height as well as percent impervious cover may not only affect the amount of water or DSi discharged by a stream but it may also affect the way a watershed responds to precipitation.

After the data were corrected for baseflow (Table 5), it became easier to investigate solely the effect of rainfall on each watershed without the baseflow signal present. Stream B did not produce any runoff during the two rain events when total rainfall reached only 0.34cm and 2.34cm, respectively. This showed the ability of wB, with less impervious cover, to retain rainwater more efficiently than wA. Watershed A produced 116.6m^3 of runoff after a light rain event that did not exceed 0.34cm of rain. During the rain event in July rainfall reached 2.34cm, and while sB discharged no runoff, sA discharged at least 406m^3 over a few hours. Interestingly enough on May 22, 2003

sB discharged more runoff per km^2 than sA after an 11.8cm rain event. Even though wA discharged less than twice as much runoff per km^2 than wB, it produced more than three times as much interflow per km^2 than wA.

During high rainfall events like the ones in April and May when rainfall reached 4.90cm and 11.8cm respectively sB discharged more interflow per m^3 of watershed than sA. During the June event sB did not discharge any interflow likely because wB had the ability to retain all the rainwater. In July there was enough rain during the sampling event to produce some interflow in wB but since the ground did not reach water saturation runoff was not produced. When rainfall was adequate to saturate both watersheds (May and June events) sB discharged significantly higher amounts of DSi per m^3 of watershed than sA. The ratio between runoff and interflow for each of the 4 rain events was always higher for sA. Stream B on every event produced more interflow than runoff.

The corrected for baseflow data in Table 5 were good evidence that the relationship between rainfall and either runoff or interflow was not simple. Each watershed responded differently to different ranges of rainfall. Watershed A for example discharged more DSi per m^3 of watershed than wB during lighter rain events but wB discharged more DSi per m^3 during heavier events. According to the CN method wA not only produced more runoff per km^2 of watershed, but it also required less rain to begin runoff production than wB. The range of rainfall height capable of producing runoff was wider for wA than for wB. According to the CN method wA started to produce runoff when rainfall reached 1.34 cm but wB didn't produce any runoff until rain exceeded 3.05 cm. This method underestimated the minimum amount of rainfall required for runoff

production in wA since a 0.34 cm event produced a significant amount of runoff according to Table 5. The number estimated for wB, however, agreed with the data collected for this study. A rainfall frequency chart constructed using 2001-2002 daily rainfall data (Figure 13) shows the number of rain events capable of producing runoff in each watershed. It is clear that almost three times as many rain events produced runoff in wA than in wB during the two years.

Since rain event frequency increases with decreasing rainfall height (Figure 13), more impervious watersheds not only produce more runoff per rain event, but they also produce runoff more often. According to this assumption, runoff production may increase exponentially in response to increasing impervious cover.

According to Table 6, 12% of the rainfall that reached the ground between January 2001 and December 2002 was discharged by wA as surface runoff, where only 2.5% was discharged as runoff by wB. This also means that the amount of DSi discharged into the ocean by wA was 12% less than it could be because of the impervious cover as the CN method estimated. Watershed B on the other hand, discharged only 2.5% less DSi than it could have due to its lower percent of impervious cover. The results obtained using the CN method strongly suggested that an overall reduction of DSi flow into coastal waters may be in fact taking place as a result of increasing impervious cover. Since DSi loads are inversely proportional to runoff loads, and since runoff loads increase exponentially with impervious cover, then long-term DSi loads may be declining exponentially in response to the increasing impervious cover.

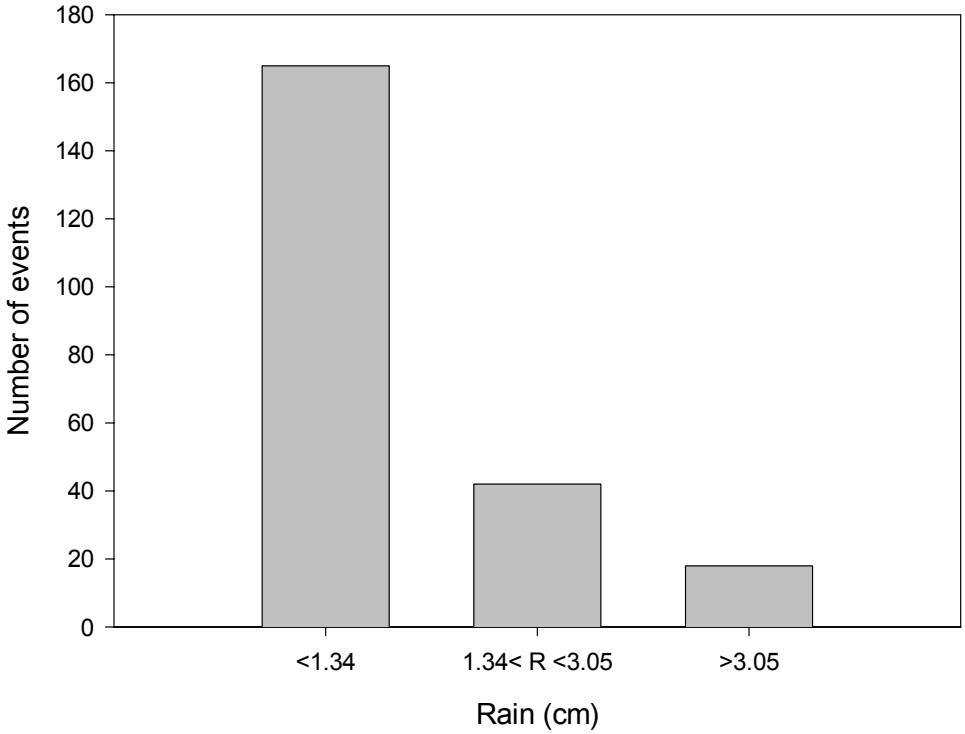

Figure 13. Rainfall frequency distribution chart for 2001-2002 rain events.

The findings of this study illustrate how two watersheds of different percent of impervious cover may affect the DSi cycle of the region and their estuaries. During rain events wA produces a relatively high volume of runoff that is released almost immediately to the estuary. This relatively large volume of DSi poor water can cause a serious short-term DSi dilution to the estuary while at the same time enriching it with N and P abundant in urban runoff. The result may be a reduction of the Si:N and Si:P ratios. Since diatom growth becomes limited when Si:N ratio becomes less than 1 the algal community composition may be altered by creating the ideal conditions for noxious algal species to flourish. In contrast, wB infiltrates and retains rainwater much more efficiently. Infiltrated water is then recharged with DSi and released over time to the estuary. During heavier rain events, even the most pristine watershed may produce surface runoff. However as in sB the runoff/interflow ratio remained relatively low and significant DSi dilution at the estuary would be avoided. Noxious algal species can also be favored by reduced estuarine flushing rates observed during rain events. According to Hales (2001) exchange rates between ocean and estuaries during rain events drop significantly as a result of the increased freshwater inflow. Rapid freshwater discharges are usually associated with high impervious cover since more pervious watersheds have the ability to retain more rainwater and release it to the stream over a longer period of time. This reduction of estuarine flushing leads to an increased residence time for materials discharged into the estuary including N and P and reduced DSi inputs from the ocean.

The volume of runoff water discharged by a stream is water that, if infiltrated would eventually carry a certain amount of DSi to the estuaries. If this amount of runoff

increases with increasing impervious cover then more water is being “wasted” as runoff and less DSi flows into the estuaries. Over a larger scale this phenomenon can cause a long-term reduction of DSi inputs into the ocean and reduce the local or even global oceanic DSi budget.

REFERENCES

Allen P, Narramore R.1985. Bedrock Controls on Stream Channel Enlargement with Urbanization, North Central Texas. American Water Resource Association 21:1037-1048.

Anderson D M. 1997. Bloom dynamics of toxic Alexandrium species in the northestern U.S. Limnology and Oceanography 42:1009-22.

Auninsh E. 1968. Hydrochemistry of Riga Gulf and river estuaries. Dissertation Thesis. Novocherkask University. 24 p.

Bannerman R, Owens D, Dodds R, Hornewer N. 1993. Sources of pollutants in Wisconsin stormwater. Water Science and Technology 28:241-259.

Banse K. 1982. Cell volumes, maximal growth rates of unicellular algae and ciliates and the role of ciliates in the marine pelagial. Limnology and Oceanography 27:1059-71.

Brzezinski M A. 1985. The Si:C:N ratio of marine diatoms: interspecific variability and the effect of some environmental variables. Journal of Phycology 21:347-357.

Bricelj V M, Londsale D J. 1997. Aureococcus anophagefferens: Causes and ecological consequences of brown tides in US mid-Atlantic coastal waters. Limnology and Oceanography 42:1023-38.

Burkholder J M, Glasgow J. 1997. Pfiesteria piscicida and other Pfiesteria-like dinoflagellates: Behavior, impacts, and environmental controls. Limnology and Oceanography 42:1052-75.

Busby W F, Lewin J. 1967. Silicate uptake and silica shell formation by synchronously dividing cells of the diatom *Navicula pelliculosa* Hilse. Journal of Phycology 3:127-131.

Cahoon L B, Hales J C, Rowland K R, Carey E S, Loucaides S, Nearhoof J E. Shellfishing closures in southwest Brunswick County, North Carolina: Septic tanks vs. storm water runoff as fecal coliform sources. In press, Journal of Coastal Research.

Cappiella K, Brown K (Center for Watershed Protection). 2001. Impervious Cover and Land Use in the Chesapeake Bay Watershed. MD: US EPA Chesapeake Bay Program Land Growth and Stewardship Subcommittee. 50 p.

Connor V.1995. Pesticide toxicity in stormwater runoff. Technical memorandum. California Regional Water Quality Control Board, Central Valley Region. Sacramento, California. 12 p.

[CWP] Center for Watershed Protection.1998. Rapid Watershed planning handbook: A Comprehensive Guide for Managing Urban Watersheds. Ellicott City, MD. 125 p.

Dartiquenave C, ECLille I, Maidment D. 1997. Water quality master planning for Austin, TX. Center of Research Water Resources. Online Report 97-6.

Doering P H, Oviatt C A, Beatty L L, Banzon V F, Rice R, Kelly S P, Sullivan B K, Frithsen J B. 1989. Structure and function in a model coastal ecosystem: silicon, the benthos, and eutrophication. Marine Ecological Progress Series 52:287-299.

Doll B, Wise-Frederick D, Buckner C, Wilkerson S, Harman W, Smith R.2000. Hydraulic geometry relationships for urban streams throughout the piedmont of North Carolina. Proceedings of the American Water Resources Association International Conference on riparian ecology and management in multi-land use watersheds. Portland, Oregon. p 299-304.

Drever J I, Zorbist J. 1992. Chemical weathering of silicate rocks as a function of elevation in the southern Swiss Alps. Geochim Cosmochim Acta 56:3209-16.

Dunne T, Leopold L B. 1978. Water in environmental planning. San Francisco: W H Freeman and Company. 818 p.

Garrels R M, MacKenzie F T. 1971. Evolution of Sedimentary Rocks. W W Norton. New York. 397 p.

Garrison D L.1979. Monterey Bay Phytoplankton 1. Seasonal cycle of phytoplankton assemblages. Journal of Plankton Research 1:241-56.

Graham L E, Wilcox L W. 2000. Algae. New Jersey: Prentice-Hall, Inc. 640 p.

Hall F R. 1968. Baseflow recessions: a review. Water Resources Research 4:973-983.

Hales J C. 2001. Tidal exchange is coastal estuaries: effect of development, rain and dredging. Master's thesis, Department of Biological Sciences, UNCW. 46 p.

Havskum H, Thingstad T F, CMIMA, Bangsholt J C, Zweifel U L, Hagstrom A, Perez M, Dolan J R. 2003. Silicate and labile DOC interfere in structuring the microbial food web

via algal-bacterial competition for mineral nutrients: Results of a mesocosm experiment. Limnology and Oceanography 48(1):129-140.

Iler R K. 1979. The Chemistry of Silica. New York: John Wiley & Sons. 866 p.

Kennedy V C. 1971. Silica variation in stream water with time and discharge. Advances in Chemistry Series 106:93-130

Klein R. 1979. Urbanization and stream quality impairment. Water Resources Bulletin 15(4):948-963.

Krauskoff K B. 1956. Dissolution and precipitation of silica at low temperature. Geochimica et Cosmochimica Acta 10:1-26.

Laznik M, Lyulko I, Zaharchenko N. 1988. Discharges of major ions, nutrients and organic matter by Latvian rivers. In: Factors of Regime Formation. Hydrometereological Processes in the USSR Seas Hydrometeoizdat, Leningrad. p 65-80.

Laznik M, Stålnacke P, Grimvall A, Wittgren H B. 1999. Riverine input of nutrients to the Gulf of Riga – temporal and spatial variation. Journal of Marine Systems 23:11-25.

Leopold L B.1968. Hydrology for urban use planning: a guidebook of the hydrologic effects of urban land use. Washington, D.C. Geological Survey Circular 554.

MacRae C. 1996. Experience from morphological research on Canadian streams: Is control of the two-year frequency runoff event the best basis for stream channel protection? In: Roesner L A. Editor. Effects of watershed development and management on aquatic ecosystems. Proceedings of the ASCE Conference. Snowbird, Utah. 596 p.

Mallin, M.A., L.B. Cahoon, M.A. Posey, D.C. Parsons, V.L. Johnson, T.D. Alphin, and J.F. Merritt. 2003. Environmental Quality of Wilmington and New Hanover County Watersheds, 2001-2002. CMS Report 03-01. Center for Marine Science, University of North Carolina at Wilmington. Wilmington, N.C.

Manning J C. 1997. Applied Principles of Hydrology. 3rd ed. New Jersey: Prentice Hall. 276p.

Neller R. 1988. A comparison of channel erosion in small urban and rural catchments, Armidale, New South Wales. Earth Surface Processes and Landforms 13:1-7.

Nilsson P, Jonson B, Swanberg I L, Sundbäck K. 1991. Response of marine shallow-water sediment system to an increased load of inorganic nutrients. Marine Ecology Progress Series 71:275-290.

Officer C B, Ryther J H. 1980. The possible importance of silicon in marine eutrophication. Marine Ecology Progress Series 3:38-91.

Otto B, Ransel K, Todd J, Lovaas D, Stutzman H, Bailey J. 2002. Paving our way to shortages: How sprawl aggregates drought. American Rivers, NRDC, Smart Growth America. 34 p.

Paerl H W.1997. Coastal eutrophication and harmful algal blooms: Importance of atmospheric deposition and groundwater as “new” nitrogen and other nutrient sources. Limnology and Oceanography 42:1154-65.

Parsons T R, Maita Y, Lalli C M.1984. A Manual of Chemical and Biological Methods for Seawater Analysis. New York: Pergammon Press. 173 p.

Peltier L. 1950. The geographic cycle in periglacial regions as it is related to climatic geomorphology. Annals of the Association of American Geographers 40: 214-36.

Rabalais N N, Turner R E, Dortch Q, Wiseman W J, Sen Gupta B K. 1996. Nutrient Changes in the Mississippi River and System Responses on the Adjacent Continental Shelf. Estuaries 19:386-407.

Rawis W J, Brakensiek D L. 1983. A procedure to predict Green Ampt infiltration parameters. Advanced Infiltration. American Society of Agricultural Engineering. 102-12.

Schelske C L, Stoermer E F. 1971. Eutrophication, silica and predicted changes in algal quality in Lake Michigan. Science 173: 423-4.

Schelske C L, Stoermer E F. 1972. Phosphorus, silica and eutrophication of Lake Michigan. In Nutrients and eutrophication. Special symposia, ed: G E Likens, 1:157-71.

Schelske C L. 2000. Diatoms as mediators of biochemical silica depletion in the Laurentian Great lakes. In: Stoermer E F, Smol J P, editors. The Diatoms: Applications for the Environmental and Earth Sciences. Cambridge: University Press. p 73-84.

Schlesinger W H. 1991. Biochemistry: An analysis of global change. San Diego: Academic Press. 443 p.

Schrader G C. 1981. Seasonal cycles of phytoplankton in relation to the hydrography of Monterey Bay. Moss Landing: Moss Landing marine laboratory. Technical publication 81-2. 34 p.

Schueler T. 1987. Controlling Urban Runoff: a Practical Manual for Planning and Designing Urban Best Management Practices. Metropolitan Washington Council of Governments. Washington, D.C. 275 p.

Simmons D L, Reynolds R J. 1982. Effects of Urbanization on Base Flow of Selected South-Shore Streams, Long Island, New York. American Water Resource Association. Water Resources Bulletin18(5): 797-806.

Smayda, T J. 1990. Novel and nuisance phytoplankton blooms in the sea: Evidence for global epidemic, p.29-40. In Toxic marine phytoplankton: Proc. 4th International Conference on Toxic Marine Phytoplankton. Elsevier.

Sournia A. 1995. Red tide and toxic marine phytoplankton of the world ocean: An inquiry into biodiversity. p 103-112. Proceedings of the 6th International Conference on toxic marine phytoplankton. Lavoisier.

Spinello A G, Simmons D L.1992. Baseflow of 10 South Shore Streams, Long Island, New York 1976-85 and the effects of urbanization on baseflow and flow duration. USGS. Water Resource Investigation Report 90-4205. 34 p.

Sundbäck K, Jonsson B. 1988. Microphytobenthic productivity and biomass in sublittoral sediments of a stratified bay southeastern Kattegat. Journal of Experimental Marine Biology and Ecology 122:63-81.

Treguer P, Nelson D M, DeMaster A J, Leynaert A, Queguiner B. 1995. The silica balance in the world ocean: a reestimate. Science 268(5209):375-80.

Trimble S.1997. Contribution of stream channel erosion to sediment yield from an urbanizing watershed. Science 278:1442-1444.

[USDA] United States Department of Agriculture, Soil Conservation Service.1986. Urban hydrology for small watersheds. Engineering Division, Technical Release 55. 164p.

[USEPA] United States Environmental Protection Agency. 1983. Results of the Nationwide Urban Runoff Program, Final report. NTIS access no. PB84-18552. Washington D.C. 200 p.

Wahdy S D, Bishara N F. 1982. In: River inputs to ocean systems. Martin J M, Burton J D, Eishma D, Editors. United Nations Environmental Program, Intergovernmental Oceanographic Commission and Scientific Committee on Oceanic Research. New York. p 311-318.

Walling D, Woodward J.1995. Tracing sources of suspended sediment in river basins: A case study of the River Culm, Devon, UK. Marine and Freshwater Research 46:324-336.

Waschbusch R, Selbig W, Bannerman R. 2000. Sources of phosphorus in stormwater and street dirt from two Urban residential basins in Madison, Wisconsin, 1994-1995. In: National conference on tools for urban water resource management and protection. US EPA February 2000:15-55